Available online at www.sciencedirect.com
SCIENCE DIRECT®
Journal of Human Evolution 46 (2004) 185–213

Curvilinear, geometric and phylogenetic modeling of basicranial flexion: is it adaptive, is it constrained?

Callum F. Ross[a]*, Maciej Henneberg[b], Matthew J. Ravosa[c,d], Simon Richard[e]

[a] *Department of Anatomical Sciences, Stony Brook University, Stony Brook, NY 11794-8081, USA*
[b] *Department of Anatomical Sciences, University of Adelaide, Adelaide, South Australia 5005, Australia*
[c] *Department of Cell and Molecular Biology, Northwestern University Feinberg School of Medicine, 303 E. Chicago Ave, Chicago, IL 60611-3008, USA*
[d] *Department of Zoology, Mammals Division, Field Museum of Natural History, 1400 South Lake Shore Drive, Chicago, IL 60605-2496, USA*
[e] *Brooklyn Union, One MetroTech Center, Brooklyn, NY 11201-3850, USA*

Received 11 July 2003; accepted 10 November 2003

Abstract

Prior work has shown that the degree of basicranial flexion among primates is determined by relative brain size, with anatomically modern humans possibly having a less flexed basicranium than expected for their relative brain size. Basicranial flexion has also been suggested to be adaptive in that it maintains a spheroid brain shape, thereby minimizing connections between different parts of the brain. In addition, it has been argued that the degree of flexion might be constrained such that increases in relative brain size beyond that seen in *Australopithecus africanus* were accommodated by mechanisms other than basicranial flexion. These hypotheses were evaluated by collating an extensive data set on basicranial flexion and relative brain size in primates and other mammals. The data were analyzed using standard least squares regression, geometric and curvilinear modeling, and phylogenetically independent contrasts (PICs). Geometric modeling does not support the hypothesis that flexion is an adaptation that facilitates enlargement of a spheroid brain. Whether humans have a less flexed basicranium than expected for their relative brain size depends on the phylogenetic vantage point from which it is evaluated. They are as flexed as expected for a descendant of the last common ancestor of the *Paranthropus–Homo* clade, but their degree of flexion cannot be predicted from the basal hominoid node, even if their relative brain size is specified. Humans undoubtedly occupy an unusual part of morphospace in terms of basicranial flexion and relative brain size, but this does not mean that their degree of flexion is or is not constrained. Curvilinear regression models and standard linear regression models describe the relationship between flexion and relative brain size equally well. Hypotheses that the degree of flexion is or is not constrained cannot be discriminated at present. Consideration of recently published ontogenetic data in the context of the interspecific data for adults suggests that much of the variance in basicranial flexion can still be explained as a mechanical consequence of brain enlargement relative to basicranial length.

Keywords: Primates; Brain; Skull; Cranial base; Ontogeny

* Corresponding author. Tel.: +1-6314446912; fax: +1-6314443947
E-mail address: cfross@ms.cc.sunysb.edu (C.F. Ross).

0047-2484/04/$ - see front matter © 2003 Published by Elsevier Ltd.
doi:10.1016/j.jhevol.2003.11.001

Introduction

The degree of flexion of the midline cranial base in primates is of interest because the cranial base is integrated with many structural and functional systems in the head (Lieberman et al., 2000). Changes in the degree of flexion therefore may impact various functional systems. Several factors have been hypothesized to be important in determining the degree of flexion, including head and neck posture, facial orientation, and brain size. The hypothesis gaining the most attention in recent years is Gould's (1977) suggestion that the degree of basicranial flexion is determined by the size of the brain relative to the length of the basicranium. Ross and Ravosa (1993) corroborated this hypothesis in interspecific comparisons across non-hominid primates. They found that as neurocranial volume relative to basicranial length increases, so the cranial base becomes more flexed (Ross and Ravosa, 1993). Subsequent work on adult primates has supported the general tenor of Gould's hypothesis, but Jeffery and Spoor's investigations reveal that in fetal primates increasing relative brain size is actually associated with decreased basicranial flexion, or flattening of the cranial base (Jeffery, 1999, 2002a, 2003; Jeffery and Spoor, 2002).

Unresolved questions fall into three groups: Is basicranial flexion adaptive or is it a mechanical consequence of brain enlargement? Are there phylogenetic effects on basicranial flexion and how do they impact on tests of the other hypotheses? Is basicranial flexion functionally constrained, as hypothesized by Ross and Henneberg (1995)?

Is basicranial flexion adaptive or a mechanical consequence of brain enlargement?

Adaptive explanations for basicranial flexion link it to three functions: reducing the energy required to support the head on an orthograde neck, improving braincase strength by maintaining its spheroid shape in context of brain enlargement, or minimizing wiring length in the brain by maintaining a spheroid brain shape. Strait and Ross (1999) have addressed the postural hypothesis elsewhere. Taking relative brain size and head posture into account, they found no evidence to suggest that variation in flexion is related to variation in head and neck orientation. Instead, relative brain size was the more important determinant of flexion. Thus, although basicranial flexion is often regarded as some kind of postural adaptation, there are no data to support this hypothesis (see also Lieberman et al., 2000).

Is basicranial flexion a mechanism for accommodating increases in relative brain size while retaining a spheroid brain shape (Ross and Henneberg, 1995; Lieberman et al., 2000)? Two possible advantages of a spheroid brain shape have been suggested. First, a spheroid brain might optimize interneuronal communication by minimizing distances between neurons (Ross and Henneberg, 1995). Minimizing of "wiring length" has been suggested to be an important design principle of neural architecture (Allman and Kaas, 1974; Barlow, 1986; Mitchison, 1991; Cherniak, 1995; Van Essen, 1997) and maintenance of a spheroid brain by increased basicranial flexion may be a way to minimize "wiring length" at the level of overall brain shape. Second, a spheroid brain might result from selection for a spheroid braincase. A spheroid braincase provides the strongest and most economical housing for the brain (Ross and Ravosa, 1993) and a spheroid braincase with a flexed base also has the advantage of reducing stresses in the poorly stress resistant region of the basicranium rostral to the occipital condyles (Demes, 1985).

Here we test the hypothesis that basicranial flexion accommodates increasing brain size relative to basicranial length in order to keep the shape of the brain and braincase spheroid. Geometric models are used to generate a variety of predictions regarding relationships between basicranial flexion, basicranial length, and brain shape in the mid-sagittal plane if sphericity in the measured neurocranial volumes is being optimized. The primate data are compared with these models and the closeness of fit between them is used to evaluate the models.

As noted above, it has been suggested that ontogenetic data from *Homo sapiens*, *Macaca nemestrina* and *Alouatta caraya* falsify the

Table 1
Abbreviations and terms used.

Landmark definitions	Angle, line and plane definitions
Ba, basion: midsagittal point on anterior foramen magnum. CP, clival point: midline point on basioccipital clivus inferior to point at which dorsum sellae curves posteriorly. FC, foramen caecum: pit on cribriform plate between crista galli and endocranial wall of frontal bone. PP, pituitary point: "the anterior edge of the groove for the optic chiasma, just in front of the pituitary fossa" (Zuckerman, 1955). PS, planum sphenoideum point: most anterosuperior midline point on sloping surface in which cribriform plate is set. S, sella: center of sella turcica, independent of contours of clinoid processes. Sp, sphenoidale: most posterior, superior midline point of planum sphenoideum.	AP: maximum anteroposterior endocranial margin of braincase diameter measured in lateral radiographs. BL1: Ba–PP+PP–Sp+Sp–PS (Ross and Ravosa, 1993; Ross and Henneberg, 1995). BL2: Ba–S+S–FC (Spoor, 1997). CBA1: Ba–S relative to S–FC (Spoor, 1997; Lieberman and McCarthy, 1999). CBA4: Ba–CP relative to Sp–PS (Lieberman and McCarthy, 1999; Ross and Ravosa, 1993). CO, clivus ossis occipitalis: endocranial line from Ba to spheno–occipital synchondrosis or CP (Ross and Ravosa, 1993). Head–neck angle: orientation of head relative to neck in locomoting animals, calculated as neck inclination relative to orbit inclination (Strait and Ross, 1999). IRE1: cube root of endocranial volume/BL 1 (Ross and Ravosa, 1993). IRE5: cube root of endocranial volume/BL 2 (McCarthy, 2001). SI: maximum superoinferior endocranial braincase diameter measured perpendicular to AP, in lateral radiographs.

hypothesis that increasing basicranial flexion is a mechanical consequence of increasing relative brain size (Jeffery, 1999, 2003; Jeffery and Spoor, 2002). Here we present all the available adult and ontogenetic data and address the issues raised by Jeffery and Spoor.

Are there phylogenetic effects on basicranial flexion?

Recent comparisons of various ways of measuring flexion and relative brain size revealed taxonomic differences in patterns of variation in basicranial flexion measures. The definitions of the different measures are given in Table 1. Analysis of variance components at different taxonomic levels (Smith, 1994) reveals that for one of the measures of relative brain size and one of the measures of basicranial flexion (IRE1 and CBA4) most of the variance is found at the family level, followed by the superfamily and then the genus levels. In contrast, for the other measures of relative brain size and basicranial flexion (IRE5 and CBA1), most of the variance is found at the Infraorder level (Lieberman et al., 2000). Adjusting degrees of freedom to account for these taxonomic effects (Smith, 1994), IRE1 and CBA4 were found to be significantly correlated with each other at $P<0.01$, as were IRE5 and CBA1. However, correlations between IRE5 and CBA4, and between IRE1 and CBA1 were only significant at $P<0.05$ (Lieberman et al., 2000). Thus, the highest correlation coefficients and degrees of significance were found between variables that showed maximum variance at the same taxonomic levels. This suggests that phylogenetic effects can affect patterns of correlation between basicranial variables and that phylogenetic relationships among primate taxa need to be accounted for in evaluating hypotheses of relationship.

Following the publication of Felsenstein's seminal 1985 paper, techniques for incorporating patterns of phylogenetic relatedness into comparative analyses have been developed and made available in the form of computer software such as CAIC, COMPARE, and PDAP (Garland et al., 1993, 1999; Garland and Ives, 2000; Blomberg et al., 2003; Rohlf, 2002). In this study the PDTREE component of the PDAP software is used to test hypotheses regarding correlations and regressions between measures of basicranial flexion and

relative brain size using Phylogenetically Independent Contrasts (PICs). To explore the importance of phylogenetic relatedness in analyzing these data, the relationships between these variables estimated using "tip" data (data from the tips of the phylogenetic tree without regard to branching pattern) are compared with the relationships estimated using PICs. In addition, the descriptive statistic, *K*, is calculated to estimate the strength of the phylogenetic signal in each variable (Blomberg et al., 2003). Various branch length options available in PDTREE are explored to determine the relative importance of tree topology and branch length on the patterns of correlation and regression measured.

Is basicranial flexion constrained?

Ross and Henneberg (1995) extended the Ross and Ravosa (1993) study to hominins and found *Homo sapiens* to be less flexed than expected. They interpreted these results as suggesting that the degree of basicranial flexion is constrained by the functional necessities of pharyngeal anatomy. This possibility arises because increased basicranial flexion among anthropoids is associated with increased facial kyphosis (Ross and Ravosa, 1993), so that as the anterior cranial base flexes ventrally relative to the posterior cranial base, so the palate (and orbits) rotate ventrally (i.e., facial kyphosis increases). Ross and Henneberg argued that the functional exigencies of pharyngeal anatomy must limit such facial kyphosis, hence constraining basicranial flexion as well. They also suggested that the brain dorsal to the notochord might preclude retroflexion of the basicranium because this would impinge upon the space available for the brain, leading them to suggest that 180 degrees might be the upper limit for basicranial flexion.

Previous debates regarding these hypotheses of constraint have focused on the methods for quantifying basicranial length and flexion (Spoor, 1997; Lieberman et al., 2000; McCarthy, 2001). McCarthy (2001) showed that basicranial length is most appropriately measured as the sum of the distance from basion to sella to foramen caecum (Basicranial length 2, or BL2 of Lieberman et al., 2000) and relative brain size is best measured using Index of Relative Encephalization 5 (IRE5). When the Ross and Ravosa flexion angle (CBA4) is regressed against IRE5, the hypothesis of constraint is confirmed: *Homo sapiens* have a less flexed basicranium than predicted (Lieberman et al., 2000; McCarthy, 2001). However, when flexion is measured using the more traditional angle defined by lines joining sella to basion and to foramen caecum, *Homo sapiens* has the degree of basicranial flexion predicted for its degree of relative encephalization (Spoor, 1997; Lieberman et al., 2000; McCarthy, 2001). Thus, for a primate with its relative brain size, *Homo sapiens'* planum sphenoideum is less flexed than expected (see above) but its foramen caecum is positioned as predicted. The meaning of these results remains to be fully explored, but it does suggest that different parts of the primate cranial base are either influenced by different factors, or by the same factors but to different degrees (Lieberman et al., 2000).

To test the hypothesis of constraint suggested by Ross and Henneberg (1995) we investigate whether CBA4 of humans is unusual for a primate of their relative brain size. In the past this has been assessed by calculating reduced major axis (RMA) lines calculated for nonhuman primates, and using the position of *Homo* relative to the estimated 95% confidence limits of those lines to assess whether the mean value for *Homo sapiens* deviates significantly from the nonhuman primate line (Ross and Henneberg, 1995; Spoor, 1997; Lieberman et al., 2000; McCarthy, 2001). Here we use a method, presented by Garland and Ives (2000), for using PICs to determine whether a species deviates from an allometric relationship. Their method calculates the prediction intervals for traits in a hypothetical species attached to a specific part of the phylogenetic tree by a specific branch length. The prediction intervals are calculated using the standard errors of the least-squares regression (LSR) calculated with PICs. When *Homo sapiens* falls inside the prediction intervals, this is taken to corroborate the hypothesis that, given their position in the primate phylogenetic tree, their degree of basicranial flexion and relative brain size are not unexpected.

We also evaluate the hypothesis of constraint on flexion by investigating nonlinear models of

the relationships between relative brain size and basicranial flexion. Various nonlinear equations describe lines with sigmoidal or logistic shapes, as predicted if the degree of flexion is limited at higher or lower relative brain sizes. We use software (CurveExpert 1.3) to search for the best curve to describe the data and compare these models with the standard linear models traditionally used in studies of basicranial evolution. Because Ross and Henneberg's hypothesis of constraint makes predictions regarding the relationship between flexion and relative brain size at small brain sizes, data on several species of nonprimate mammals are included in these curvilinear analyses.

Methods

Sample

The core of the data on basicranial flexion and relative brain size were collected previously (Ross and Ravosa, 1993; Ross and Henneberg, 1995; Strait and Ross, 1999; Lieberman et al., 2000). The complete data set consists of 64 species of living primates, three fossil primate specimens, and 31 species of non-primate mammals (Table 2). The primates, tree shrews and dermopterans were grouped as euarchontans following Murphy et al. (2001).

Radiographic methods

The non-primate mammal and primate specimens were radiographed at the American Museum of Natural History, the Field Museum of Natural History, the Museum of Comparative Zoology at Harvard University, and the British Museum of Natural History using portable x-ray machines. Each specimen was placed directly on the radiographic film, aligned with its midsagittal plane parallel with the film. The collimeter of the x-ray machine was positioned one meter above the film and aligned perpendicular to the film. To correct for radiographic enlargement the linear measures taken from each radiograph were corrected by multiplying them by the ratio:

$$\frac{\text{prosthion–basion length measured on the skull}}{\text{prosthion–basion length measured on the radiograph}}$$[1]

Measurement of flexion and relative brain size

CBA1 is the inferior angle between the lines running from sella to basion and sella to foramen caecum (Fig. 1). CBA4 is the inferior angle between the endocranial surfaces of clivus planum sphenoideum and the occipital clivus. Data on CBA1 were gathered from the original radiographs measured by Ross and Ravosa (1993) and Ross and Henneberg (1995), as well as from the newly acquired radiographs. Data on CBA4 were taken from the data set of Ross and Ravosa (1993) and Strait and Ross (1999). New data from previously unsampled taxa were gathered following the methods of Ross and Ravosa (1993).

Linear measures of endocranial basicranial length were taken from the lateral radiographs. Following McCarthy (2001), basicranial length was estimated using BL2, the sum of the distances basion–sella and sella–foramen caecum. Data on fossil taxa were derived from Spoor (1997): raw data on flexion, BL and neurocranial volume were supplied to CFR by Spoor (pers. comm.).

The volume of the neurocranium was measured using mustard seed or taken from the literature. The Index of Relative Encephalization 5 (IRE5) for each specimen was calculated as

$$\frac{\sqrt[3]{\text{neurocranial volume}}}{\text{BL2}}$$

Does basicranial flexion facilitate spheroid enlargement of the brain?

Ideally sphericity would be measured in three dimensions, but because only lateral radiographs were available for most taxa, the relationship between sphericity and flexion was evaluated using midline measures of shape. An estimate of sphericity of the neurocranium in lateral projection was

[1] Note the correction to the formula published in Ross and Henneberg (1995), where the numerator and deonimator were inverted.

Table 2
Means of Cranial Base Angles 1 and 4 (CBA1, CBA4), anteroposterior (AP) and superoinferior (SI) diameter of the braincase, BL2 and neurocranial volume and Index of relative Encephalization 5 (IRE5) for the taxa included in this study. All measures are degrees, centimeters, and cubic centimeters

Species	n	CBA4	CBA1	AP	SI	BL2	Brain volume	IRE5
Alouatta belzebul	5	186	183	6.07	3.51	5.96	50.83	0.622
Alouatta palliata	5	188	181	6.17	3.55	5.78	52.50	0.648
Aotus trivirgatus	6	180	177	4.04	2.43	3.23	18.33	0.817
Arctocebus calabarensis	5	168	194	3.31	1.85	3.04	7.20	0.635
Ateles fusciceps	5	162	170	7.59	4.76	5.56	106.33	0.852
Avahi laniger	5	180	184	3.65	2.02	3.18	10.33	0.684
Brachyteles arachnoides	7	161	173	7.40	4.87	5.84	112.40	0.827
Cacajao calvus	6	172	168	6.55	4.35	4.74	70.50	0.871
Callicebus moloch	6	176	176	4.06	2.45	3.50	17.50	0.743
Callimico goeldii	5	171	165	3.77	2.25	2.96	12.17	0.777
Callithrix argentata	5	164	165	3.31	2.01	2.74	8.33	0.741
Cebuella pygmaea	5	162	164	2.41	1.57	2.24	5.00	0.765
Cebus apella	5	173	167	6.23	4.01	4.87	63.83	0.821
Cercocebus torquatus	6	172	157	7.04	4.53	5.54	97.83	0.832
Cercopithecus mitis	5	179	170	6.49	3.94	5.17	70.67	0.799
Cheirogaleus major	5	181	187	3.29	1.52	3.14	5.75	0.570
Chiropotes satanas	6	170	170	6.03	3.83	4.50	55.67	0.848
Chlorocebus aethiops	5	171	165	6.15	3.98	4.74	63.00	0.839
Daubentonia madagascarensis	5	157	169	5.55	3.22	3.27	43.20	1.073
Erythrocebus patas	6	167	159	7.55	4.56	5.78	100.20	0.804
Eulemur fulvus	6	171	184	4.94	2.61	4.45	23.33	0.642
Euoticus elegantus	6	158	178	3.26	1.69	2.74	5.67	0.651
Gorilla gorilla	5	148	157	11.02	7.45	9.19	489.60	0.858
Hapalemur griseus	6	175	180	4.17	2.17	3.70	13.25	0.640
Homo sapiens	48	112	138	16.08	13.01	8.93	1351.00	1.184
Hylobates lar	6	153	168	6.84	4.59	5.51	97.67	0.835
Hylobates moloch	6	160	173	6.58	4.22	5.24	89.17	0.853
Indri indri	5	168	186	5.71	2.91	5.44	34.67	0.600
Lagothrix lagothricha	6	176	176	7.20	4.47	5.59	96.33	0.819
Lemur catta	5	176	179	4.54	3.17	4.19	24.50	0.693
Leontopithecus rosalia	6	173	173	3.79	1.93	3.05	12.33	0.758
Lepilemur mustelinus	6	178	181	3.49	1.82	2.57	8.67	0.798
Lophocebus albigena	6	163	162	7.23	4.45	5.48	101.50	0.851
Loris tardigradus	6	162	187	2.89	1.76	2.35	6.50	0.793
Macaca fascicularis	4	166	165	6.24	6.24	4.76	66.50	0.852
Macaca nigra	6	158	151	6.85	4.61	5.44	85.17	0.809
Macaca sylvana	4	154	159	7.27	4.65	5.60	102.00	0.835
Mandrillus leucophaeus	1	160	155	8.73	5.82	7.20	187.00	0.794
Mandrillus sphinx	6	154	153	8.57	5.51	6.65	152.00	0.803
Miopithecus talapoin	5	168	164	5.25	3.26	3.60	41.33	0.960
Mirza coquereli	1	158	189	3.18	1.59	3.02	5.00	0.567
Nycticebus coucang	6	171	186	3.60	2.07	3.39	10.67	0.649
Otolemur crassicaudatus	6	167	179	4.23	2.21	3.83	12.33	0.603
Pan paniscus	1		148	9.59	7.15	7.15	335.00	0.972
Pan troglodytes	6	152	159	10.82	7.13	8.07	398.33	0.911
Papio anubis	6	154	153	8.28	5.60	6.57	165.33	0.835
Papio hamadryas	7		155	9.04	6.93	7.17	170.50	0.773
Piliocolobus badius	6	156	167	6.57	4.14	5.19	70.83	0.798
Pithecia pithecia	6	182	176	5.16	3.20	4.36	34.00	0.744
Pongo pygmaeus	5	135	161	9.96	7.26	8.61	396.83	0.854
Presbytis melalophos	6	154	161	6.34	3.99	4.71	68.00	0.866

Table 2 (continued)

Species	n	CBA4	CBA1	AP	SI	BL2	Brain volume	IRE5
Presbytis rubicunda	6	152	159	6.40	4.02	4.82	74.67	0.873
Procolobus verus	5	157	171	5.93	3.71	4.69	55.80	0.815
Propithecus verreauxi	5	168	185	5.12	2.76	4.56	29.67	0.679
Pygathrix nemaeus	6	145	156	6.55	4.18	5.07	84.71	0.866
Rhinopithecus roxellana	6	150	157	7.23	4.46	5.39	111.00	0.892
Saguinas fuscicollis	5	170	165	3.35	1.97	2.74	8.67	0.749
Saimiri sciureus	6	169	166	4.70	2.91	3.27	23.33	0.873
Semnopithecus entellus	6	148	160	6.80	4.51	5.50	87.33	0.807
Simias concolor	6	161	160	5.89	4.25	4.82	55.50	0.792
Symphalangus syndactylus	6	167	174	7.70	4.65	6.50	129.17	0.778
Tarsius syrichta	1	141	151	2.71	1.83	2.09	4.00	0.760
Theropithecus gelada	6	152	157	7.65	5.02	6.02	127.50	0.836
Trachypithecus cristatus	6	166	168	6.29	3.93	5.31	64.83	0.757
Varecia variegata	5	177	188	5.44	2.77	5.12	32.67	0.624
KNM-WT 17000	1	115	156			8.40	410.00	0.880
OH5	1	NP[1]	135			8.25	530.00	0.980
Sts 5	1	112	147	11.94	9.75	7.84	485.00	1.002
Cynocephalus volans	6	176	188	4.10	2.35	4.13	7.12	0.466
Tupaia glis	3	184	188	2.80	1.51	2.55	3.13	0.573
Urogale everetti	5	184	179	3.47	1.77	2.91	4.44	0.565
Petrodromus tetradactylus	6	186	189	3.09	1.61	2.73	2.98	0.527
Rhynocyon cirnei	6	192	180	3.64	1.88	3.26	4.97	0.523
Procyon lotor	5	179	195	6.86	4.02	6.50	53.80	0.581
Arctictis binturong	4	167	198	6.55	3.65	6.69	40.75	0.515
Herpestes sanguineus	5	191	208	3.90	1.97	4.10	8.20	0.492
Ailurus fulgens	5	166	194	6.07	4.27	5.74	42.40	0.607
Caluromys philander	6	187	192	2.76	1.61	2.78	2.83	0.509
Caluromys irrupta	2	181	195	3.49	1.73	3.56	3.90	0.442
Caluromys derbianus	5	161	195	3.24	1.41	3.19	3.46	0.474
Philander opossum	5	175	184	3.48	1.56	3.77	3.76	0.412
Petrogale lateralis	5	185	191	5.70	3.36	5.22	17.80	0.500
Ratufa indica	6	182	192	4.72	2.30	4.73	11.50	0.477
Sciurus carolensis	5	182	192	3.71	2.07	3.66	7.42	0.533
Lepus townsendi campanius	5	148	186	4.95	2.67	4.63	12.60	0.502
Pronolagus rupestris	5	158	177	4.57	2.51	4.11	10.14	0.526
Brachylagus idahoensis	6	145	178	3.32	2.12	3.00	4.57	0.554
Oryctolagus cuniculus	6	142	177	4.89	2.52	4.46	9.52	0.475
Sylvilagus audobonii	8	138	175	3.98	2.49	3.66	7.31	0.530
Ochotona rufescens regina	5	143	172	3.13	1.48	2.98	2.02	0.424
Pteropus hypomelanus lutens	6	152	175	3.56	2.12	3.57	5.73	0.502
Rousettus aegyptiacus leachi	7	165	185	2.35	1.55	2.22	2.11	0.577
Hipposideros commersoni	5	166	186	1.93	1.07	1.70	0.94	0.577
Didelphis virginiana	3	178	185	4.97	2.03	5.15	7.33	0.377
Zaglossus	3	186	180	6.16	3.20	5.23	35.67	0.630
Tachyglossus aculeatus	6	192	185	4.88	2.64	4.14	19.33	0.648
Oreotragus oreotragus	5	155	199	8.10	5.81	7.82	55.20	0.487
Ourebia ourebia goslingi	4	154	198	8.44	6.36	8.26	57.25	0.467
Madoqua guentheri	7	158	178	6.18	4.95	6.30	26.71	0.475

[1]NP, not preserved.

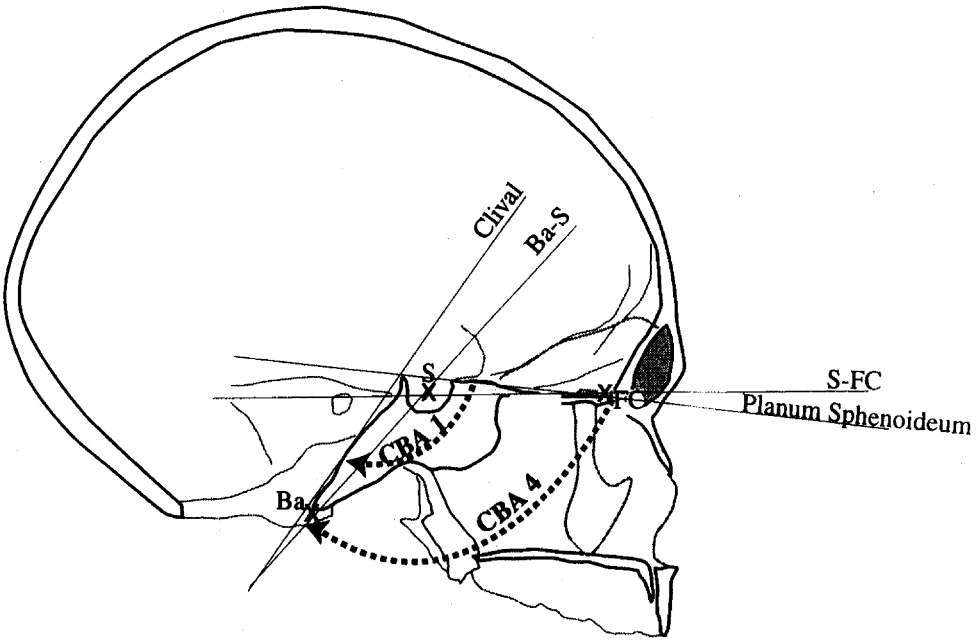

Fig. 1. Diagram of mid-sagittally sectioned skull of *Homo sapiens* illustrating points and planes used to measure the cranial base angles 1 and 4 (CBA1 and CBA4) and basicranial length. Ba, basion, S, sella, FC, foramen caecum, clival=clival plane.

calculated from the lateral radiographs. Maximum anteroposterior (AP) diameter of the braincase was measured first, then maximum superoinferior (SI) braincase diameter was measured in a plane perpendicular to the maximum AP measure (Fig. 2a). To determine whether basicranial flexion accommodates increasing brain size relative to basicranial length in order to keep the shape of the brain and braincase spheroid, two approaches were taken.

First, it was investigated whether the changes in flexion and the AP/SI measure of shape matched those predicted by a circular/semi-circular geometric model. A semicircle has a flat base with a flexion angle of 180 degrees, and a ratio of AP diameter to "SI" diameter of 2.0 (Fig. 2c). As the base flexes about its center the SI diameter will increase as CBA decreases (Fig. 2b), according to the following equation:

$$SI = AP/2 + (AP/2 * \sin(180 - CBA)) \quad (1)$$

Therefore, when CBA=180 degrees, SI diameter is expected to be half that of AP (and the AP/SI ratio=2.0) and when CBA=90 degrees, SI will equal AP and the ratio=1. If cranial base flexion maintains sphericity in the midsagittal plane, it should change as a function of the AP/SI ratio according to Equation (1). CBA1 and CBA4 were both plotted against AP/SI, along with the function in Equation (1), and the observed versus the predicted visually compared.

Second, the relationship between basicranial flexion and relative brain size across primates was compared to the equation describing the relationship between the volume of a partial sphere (V), the radius of that sphere (r), and the angle subtended by the segment of the sphere that is "missing" (θ) (Fig. 2b).

$$\theta = \left\{ 2\pi - \frac{3}{2r^3} V \right\} \quad (2)^2$$

The CBA predicted by Equation (2) was calculated using half the maximum anteroposterior

[2] See Appendix A for the derivation of this equation.

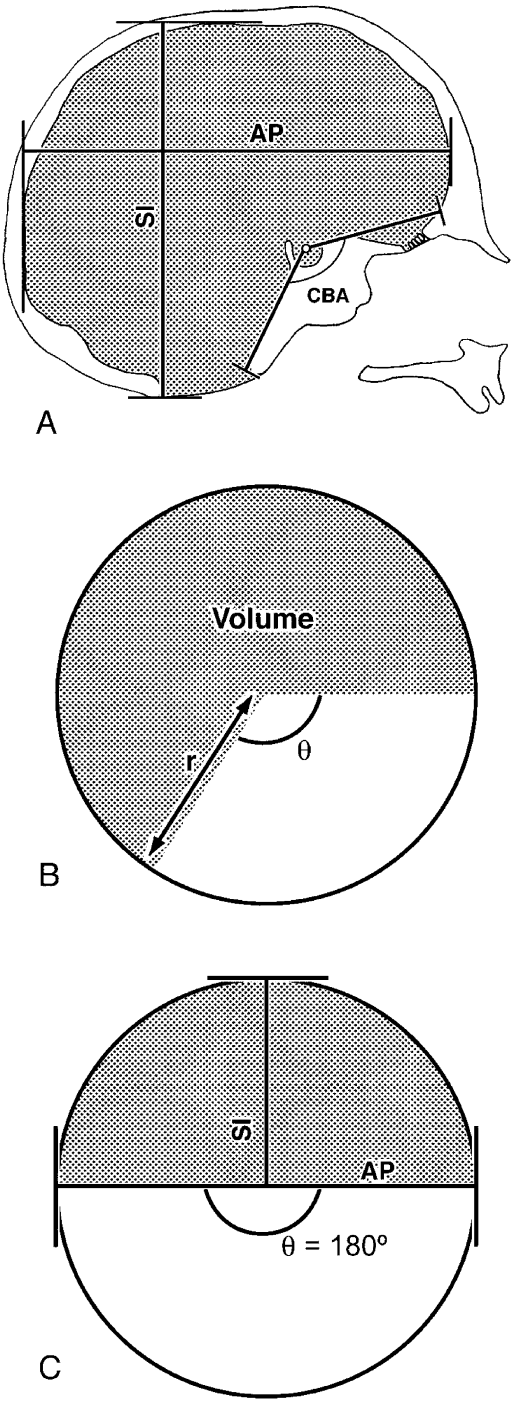

diameter of the neurocranial cavity as an estimate of r, and neurocranial volume as an estimate of V. Both CBA and θ were plotted against IRE on the same graph and visually compared. The error of the model was estimated using the standard error of the estimate (Sokal and Rohlf, 1981).

Phylogenetic effects on basicranial flexion

Phylogenetic effects on basicranial flexion in euarchontans were investigated using the PDTREE component (Garland et al., 1999; Garland and Ives, 2000) of the Phenotypic Diversity Analysis Programs (PDAP) Version 6.0 (Garland et al., 1993; Garland et al., 2002). The phylogenetic tree illustrated in Fig. 3 was imported into the PDTREE component of PDAP along with the measures of flexion and relative brain size in euarchontans (Table 2). PDTREE was used to analyze the relationship between flexion and relative brain size using Felsenstein's (Felsenstein, 1985) method of PICs and these results compared with those calculated using "tip" data. PICs are calculated as the difference between the values of a trait in two sister taxa ("tip" species or internal nodes of a phylogenetic tree) divided by the square root of the sum of their branch lengths. When using PICs, branch lengths are assumed to be proportional to the expected variance of evolution in the traits in question (Felsenstein, 1985) and these branch lengths must be tested for "statistical adequacy" and transformed if they do not meet this criterion (Garland et al., 1992; Blomberg et al., 2003). In particular, contrasts over longer branch lengths are expected to be greater and therefore given greater weight in regression or correlation analyses (Garland et al., 1992). To mitigate this effect, each independent contrast is standardized by dividing it by the square root of the sum of its

Fig. 2. Diagram illustrating measures taken in testing spheroid hypothesis. The spheroid hypothesis is tested by modeling the skull as a sphere partially occupied by neurocranial cavity. The base of the skull is represented by lines used to measure flexion, with the length of the basion–sella–foramen caecum lines representing the length of the skull base. The anteroposterior (AP) and superoinferior (SI) measures of the neurocranium are used to test for sphericity. AP/2 is used as an estimate of the sphere radius.

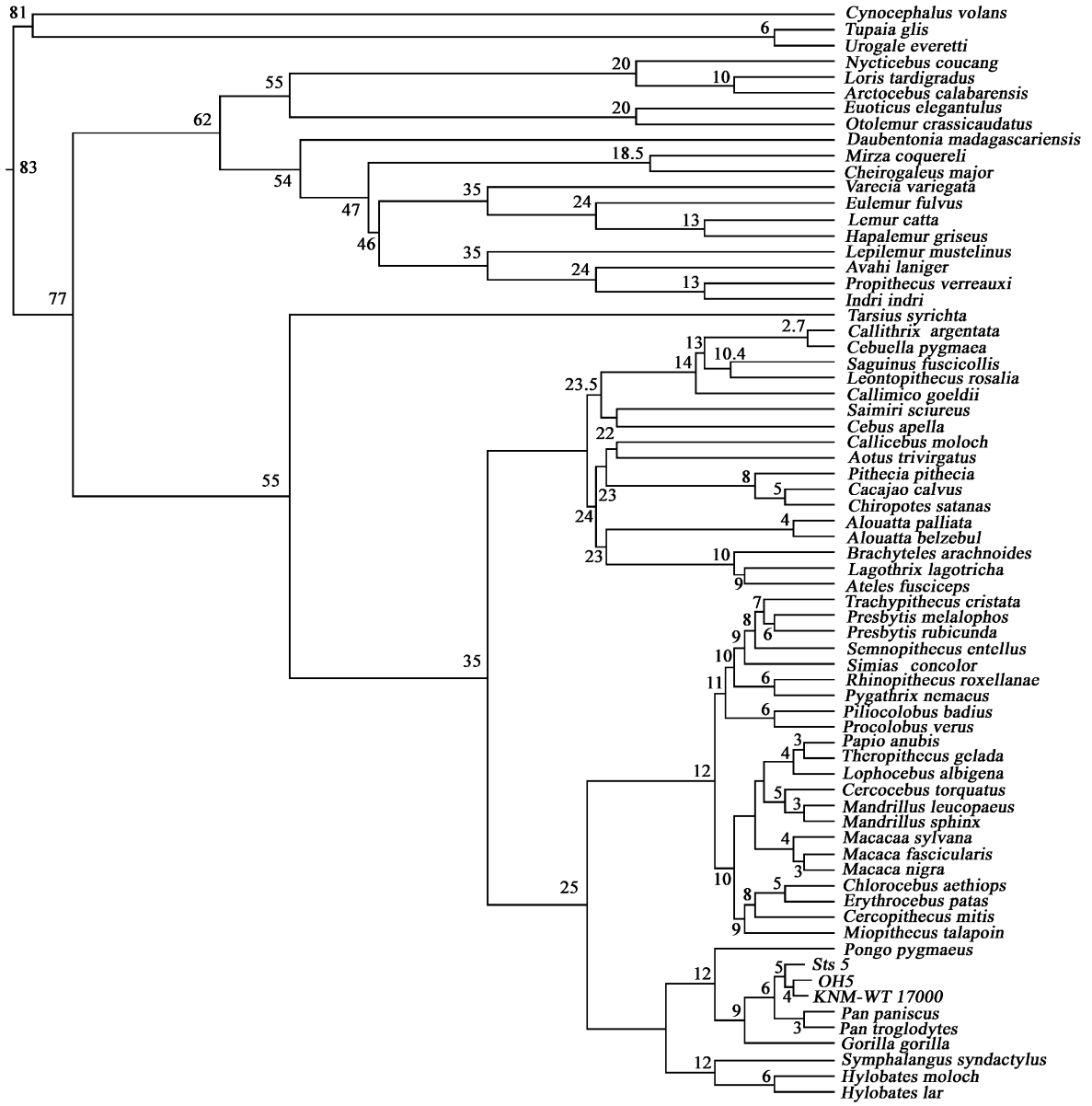
Cynocephalus volans
Tupaia glis
Urogale everetti
Nycticebus coucang
Loris tardigradus
Arctocebus calabarensis
Euoticus elegantulus
Otolemur crassicaudatus
Daubentonia madagascariensis
Mirza coquereli
Cheirogaleus major
Varecia variegata
Eulemur fulvus
Lemur catta
Hapalemur griseus
Lepilemur mustelinus
Avahi laniger
Propithecus verreauxi
Indri indri
Tarsius syrichta
Callithrix argentata
Cebuella pygmaea
Saguinus fuscicollis
Leontopithecus rosalia
Callimico goeldii
Saimiri sciureus
Cebus apella
Callicebus moloch
Aotus trivirgatus
Pithecia pithecia
Cacajao calvus
Chiropotes satanas
Alouatta palliata
Alouatta belzebul
Brachyteles arachnoides
Lagothrix lagotricha
Ateles fusciceps
Trachypithecus cristata
Presbytis melalophos
Presbytis rubicunda
Semnopithecus entellus
Simias concolor
Rhinopithecus roxellanae
Pygathrix nemaeus
Piliocolobus badius
Procolobus verus
Papio anubis
Theropithecus gelada
Lophocebus albigena
Cercocebus torquatus
Mandrillus leucopaeus
Mandrillus sphinx
Macacaa sylvana
Macaca fascicularis
Macaca nigra
Chlorocebus aethiops
Erythrocebus patas
Cercopithecus mitis
Miopithecus talapoin
Pongo pygmaeus
Sts 5
OH5
KNM-WT 17000
Pan paniscus
Pan troglodytes
Gorilla gorilla
Symphalangus syndactylus
Hylobates moloch
Hylobates lar

branch lengths. The adequacy of this method of standardization can then be tested by plotting the standardized independent contrasts against their standard deviations (Garland et al., 1992). Any trends in these plots indicate that contrasts are not adequately standardized and some kind of transformation is required.

In this study, we used four different branch length sets and tested their standardization using the methods just described. *Real* branch lengths were calculated from divergence dates estimated by molecular clock and fossil data sets (Yoder et al., 1996; Porter et al., 1997; Yoder, 1997; Chaves et al., 1999; Page et al., 1999; Hartwig, 2002; Eizirik et al., 2003). The standardized contrasts using these branch lengths were found to be significantly correlated with their standard deviations, so these real branch lengths were transformed into $\log_{10}$ and tested to demonstrate that they met the assumptions of the statistics. The second branch length set was constant branch lengths in which all branches in the tree were assigned a length of 1.0. The third set were Pagel's (Pagel, 1992) arbitrary branch lengths, in which all internode segments are set equal to one but tips are constrained to be contemporaneous. The fourth set were Grafen's (Grafen, 1989) arbitrary branch lengths in which the tips are contemporaneous and the depth of each node equals one less than the number of species that descend from it. These latter three branch length sets were found to be adequately standardized.

The practical effect of phylogenetic relatedness on the euarchontan regression equations was determined by comparing the least-squares regression (LSR) equation calculated using PICs (forced through the origin) with the LSR equation calculated using the "tip" data. Significance of differences was assessed by determining whether the slopes and intercepts of the PIC LSR lines,

Fig. 3. Phylogenetic tree of euarchontans used in this study. The PDTREE files are available from CFR upon request. Numbers are ages of nodes in million years. Ages of Primates (Scandentia+*Cynocephalus*) node (83 Myr), basal Primates node (77 Myr), *Tupaia–Urogale* node (7 Myr) from Eizirik et al. (2003).

Branching times for basal strepsirrhine nodes, Strepsirrhini (62 Myr), *Daubentonia*–Lemuriformes (54 Myr), non-*Daubentonia* Malagasy lemurs (47 Myr) are from Yoder et al. (1996) and Yoder (1997). There is a discrepancy between Eizirik et al.'s model and Yoder's, with Yoder accepting an age of 63 Myr for the basal primate node, then 62 Myr for Strepsirrhini. The net effect of combining the old basal euarchontan node estimates of Eizirik et al. with the young basal strepsirrhine node estimates of Yoder is to lengthen the basal branch of Strepsirrhini. Within Malagasy strepsirrhines, clades are difficult to date. Accepting Yoder's (Yoder, 1997) suggestion that the major clades diverged immediately after colonization, we split the clade divergence times evenly between 46 and the present. The two cheirogaleids are hypothesized to have split at half Yoder's minimum age (37 Myr) for the basal Malagasy radiation (18.5 Myr)

The basal lorisiform divergence into galagids and lorisids is set at 55 Myr (Yoder, 1997), consistent with recent fossil discoveries by Seiffert et al. (2003) of a lorisid and a galagid from late middle Eocene deposits dated at 41.2–36.9 Myr. The extant radiations of lorisids and galagids are set at 20 Myr because these are the earliest fossils (Phillips and Walker, 2002). The divergence of *Arctocebus* and *Loris* is set at 10 Myr, half way between 20 Myr and the present.

The basal node for Haplorhini was estimated at (55 Myr) based on the presence of fully fledged tarsiers, *Tarsius eocaenus* at 45 Myr (Beard et al., 1996) (see also Ross, 2003); platyrrhine–catarrhine split is based on fossil evidence (Hartwig, 2002) and molecular clock (Eizirik et al., 2003) at 35 Myr; hominoid cercopithecoid split at 25 Myr is based on fossil evidence (Gingerich, 1984; Goodman et al., 1998; Fleagle, 1999). Branching patterns within Cercopithecoidea are based on Jablonski's (Jablonski, 2002) summary of fossil and molecular evidence. The split between the great ape+human clade and the clade of lesser apes at 16 Myr, the split between *Pongo* and the African ape+human clade at 13 Myr, the *Gorilla–Pan+Homo* split (9 Myr), and the *Homo–Pan* split at 6 Myr are all based on the summaries of Begun (2002) and Pilbeam (2002). The split within *Pan* at 3 Myr is from Porter et al. (1997) and within *Hylobates* at 6 Myr from Eizirik et al. (2003). The *Australopithecus africanus+Homo sapiens* lineage is modeled as diverging from the OH5+WT17000 clade at 5 Myr, and the OH5 and WT17000 lineage splitting at 4 Myr. As noted in the text, *Homo sapiens* is modeled as splitting from the *A. africanus* lineage at 4 Myr, 1 Myr prior to the appearance of *A. africanus*.

The platyrrhine divergence dates are based on a rapid basal divergence date around 25 Myr (Porter et al., 1997) and a conventional phylogeny with *Callimico* as sister taxon to the two-molared callitrichines. Divergence dates for *Cebuella–Callithrix* (2.7 Myr), *Leontopithecus–Saguinus* (10.4 Myr), and basal callitrichines (14 Myr) are derived from Chaves et al. (1999); pitheciines (8 Myr), atelines (10.2 Myr); *Alouatta* (4 Myr), *Cacajao–Chiropotes* (5 Myr) are from (Porter et al., 1997). Dolichocebus was accepted as a *Saimiri* relative, dating the *Cebus–Saimiri* divergence to 22 Myr; the divergence of the *Cebus–Saimiri* clade from the callitrichine clade was taken has 23.5 Myr, half the time between the platyrrhine root (25 Myr) and and 22 Myr. Similarly, *Tremacebus* is accepted as an aotine, dating the *Aotus–Callicebus* divergence to the Early Miocene (also consistent with callicebine affinities for *Carlocebus*): 22 Myr was chosen arbitrarily. This clade joins the pitheciin clade 1 Myr earlier (23 Myr), with atelines 1 Myr earlier than that (24 Myr), then to the platyrrhine root at 25 Myr.

mapped back into the original data space (Garland and Ives, 2000), lie within the 95% confidence limits of the equations calculated using tip data.

The strength of the phylogenetic signal in each variable was estimated using the K statistic of Blomberg et al. (2003), calculated in MATLAB using software PHYSIG.M provided by T. Garland. The K statistic measures "the amount of phylogenetic signal relative to the amount expected for a character undergoing Brownian motion evolution along the specified topology and branch lengths" (Blomberg et al., 2003: 730). The amount of phylogenetic signal is measured as the ratio of the mean squared error of the tip data relative to the phylogenetically corrected mean (MSE_0), divided by the mean squared error of the data relative to the variance–covariance matrix derived from the tree in question (MSE). This is the observed MSE_0/MSE. This value is then scaled by dividing it by the expected MSE_0/MSE, i.e., the MSE_0/MSE expected under Brownian motion evolution along the specified tree topology. Thus,

$$K = \frac{\text{observed } MSE_0/MSE}{\text{expected } MSE_0/MSE}$$

A trait with a K value of 1.0 on a tree means that the trait shows exactly the degree of phylogenetic signal expected under a Brownian motion model of evolution on that tree. K values of less than 1.0 indicate either that the trait did not evolve in a Brownian fashion, perhaps because of adaptation of the trait in some parts of the tree and not others, or that there is measurement error in the trait, the tree topology or the branch lengths. Together these factors combine to make close relatives look less similar than under a pure Brownian motion model of evolution (Blomberg et al., 2003). K values of greater than 1.0 suggests that close relatives are more similar than expected under a pure Brownian motion model of evolution.

To determine whether *Homo sapiens* deviate from the relationship between relative brain size (IRE5) and basicranial flexion (CBA1 and CBA4) characteristic of other euarchontans, PDTREE was used to determine whether *Homo* lies outside the prediction limits of the LSR equations calculated from the PICs and forced through the origin then transformed back into the original data space (Garland and Ives, 2000). First it was determined whether the values for CBA1, CBA4 and IRE5 observed in *Homo sapiens* fell within the 95% prediction intervals generated for the euarchontan tree. Two kinds of prediction intervals are calculated: generic and specific. *Generic prediction intervals* are those calculated without specifying the phylogenetic position of the hypothetical species (in this case, *Homo sapiens*) being predicted. This is computationally equivalent to and achieved by predicting the values for a species attached to the root of the tree by a branch of specified length (real branch length=$\log_{10}$ of 83 Myr [7.919], the age of the (primate–treeshrew+flying lemur) divergence; constant branch length=1.0, Pagel and Grafen branch lengths=average branch length for entire tree). *Homo-specific prediction intervals* are those calculated when the phylogenetic position of the hypothetical species to be predicted is specified. In PDTREE, this is achieved by rerooting the tree along the branch to which the hypothetical species is attached and specifying the length of the branch. This procedure displaces the intercept of the LSR line towards the estimated value for the new tree root; i.e., the value at the node to which *Homo sapiens* is attached. In calculating the *Homo-specific prediction intervals* using real branch lengths, the length of the branch leading to *Homo sapiens* was assumed to be 4 Myr long and attached 1 Myr below the Sts 5 tip. (The $\log_{10}$ of 4 (6.602) was used as the branch length). In the case of constant branch lengths, the branch leading to *Homo* was given a branch of 1.0. The branch lengths for the Pagel and Grafen branch length sets were taken as the averages of all the branch lengths in those trees. In this way it is determined whether the values observed in *Homo sapiens* are expected for a euarchontan attached either to the base of the tree by an 83 Myr branch length, or to the branch leading to Sts 5 by a 4 Myr branch length.

In addition to determining whether both basicranial flexion and relative brain size in *Homo sapiens* match those expected for a euarchontan, it was also determined whether the degree of flexion observed in *Homo sapiens* matched that predicted for a euarchontan with its relative brain size. Once again, both *Generic* and *Homo-specific prediction*

intervals were calculated, assuming a basal placement of the *Homo* branch and a placement on the branch leading to Sts 5.

Is basicranial flexion constrained?

To test the hypothesis that CBA4 varies as a function of IRE5, but with the degree of flexion constrained to lie between 180 and 90 degrees, various sigmoidal, polynomial, exponential, power law and quadratic functions, many with upper and/or lower asymptotes, were fit to the data using CurveExpert 1.3. Curve Expert uses the Levenberg–Marquardt algorithm to search for the values of the equations that minimize error about the lines. The standard errors of the estimate about the calculated equations were compared with that about the linear least squares line and the spheroid model (Equation (2)) using the *F*-test.

Results

Raw data

The mean values for all taxa used in this study are given in Table 2.

Does basicranial flexion facilitate spheroid enlargement of the brain?

Do changes in flexion and the AP/SI measure of shape match those predicted by a circular/semicircular geometric model? In Fig. 4 the braincase shape ratio AP/SI is plotted against the two measures of flexion, CBA1 and CBA 4. Also plotted is the relationship between the AP/SI ratio and the CBAs expected under the geometric model (Equation (1)). Although in neither case do the observed relationships very closely match that predicted by geometry, the line of geometric expectation is met significantly better by CBA4 (standard error of estimate=0.340) than CBA1 distribution (standard error of estimate=0.463). This suggests that CBA4 is better than CBA1 for evaluating hypotheses regarding spheroid enlargement of the brain.

Fig. 5A plots both θ (the cranial base angle predicted by the geometric model described in

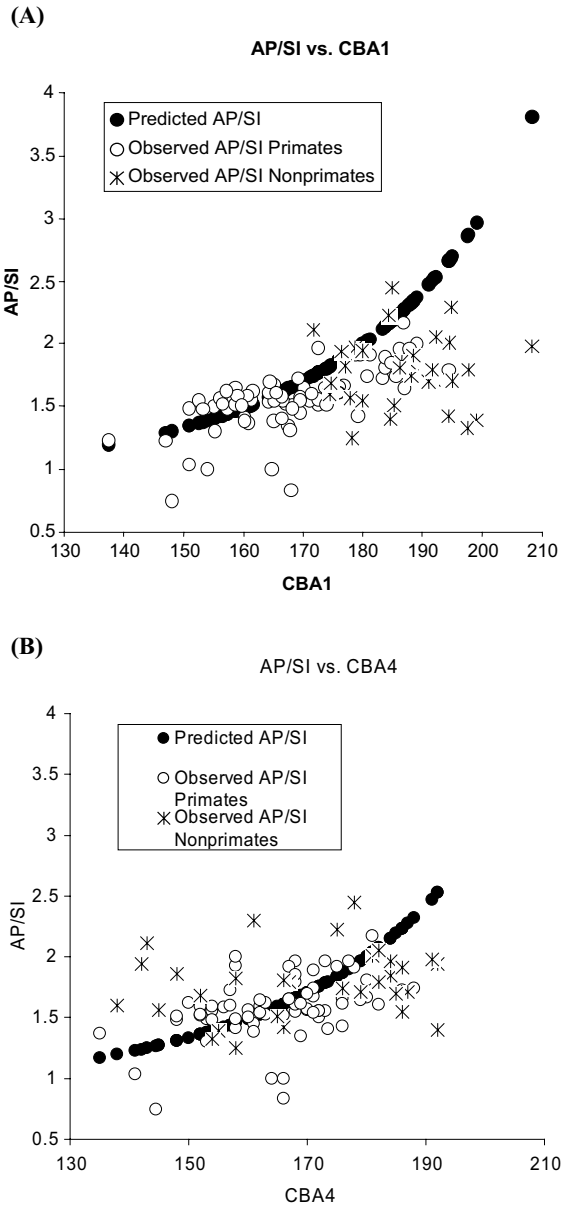

Fig. 4. Bivariate plots of AP/SI ratio against (A) CBA1 and (B) CBA4.

Equation (2)) and the observed CBA4 against IRE5 across all taxa measured. Fig. 5B plots values for θ such that $180>\theta>90$, as predicted by the constraint model of Ross and Henneberg (1995). The geometric model does a poor job of predicting CBA4 at small values of IRE5 (below

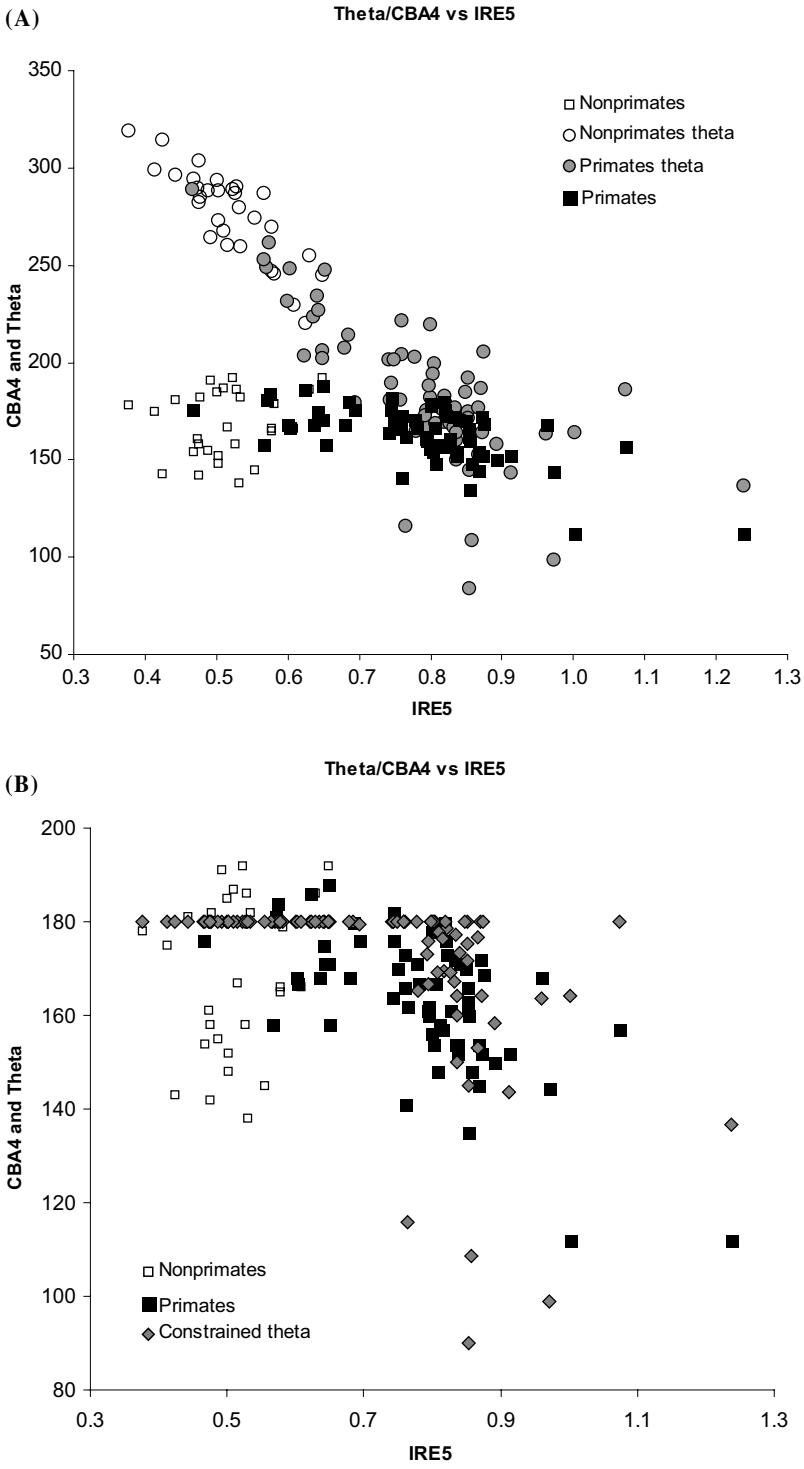

Fig. 5. Bivariate plots against IRE5 of actual CBA4 measured, (A) theta predicted by Equation (1), and (B) theta constrained to lie between 180 and 90 degrees.

Table 3
Least-squares regression statistics for both CBA1 and CBA4 against IRE5 across Euarchonta.

Flexion measure	CBA1	CBA1	CBA1	CBA1	CBA4	CBA4	CBA4	CBA4
Data source	Tips	PICs	PICs	PICs	Tips	PICs	PICs	PICs
Branch lengths	NA	Real (log_{10})	Constant	Pagel	NA	Real (log_{10})	Constant	Pagel
n	69	69	69	69	68[1]	68	68	68
R	−0.769	−0.506	−0.501	−0.465	−0.576	−0.350	−0.348	−0.309
Slope	−81.440	−42.720	−41.745	−45.129	−72.398	−41.741	−40.616	−42.404
Standard Error	8.279	8.901	8.670	10.495	12.652	13.728	13.449	16.050
Lower 95% CI	−97.965	−60.487	−59.110	−66.077	−97.659	−69.149	−67.468	−74.451
Upper 95% CI	−64.915	−24.953	−24.380	−24.180	−47.138	−14.332	−13.763	−10.359
Generic Intercept	232.287	204.539	203.836	205.012	219.741	195.180	194.226	195.386
Standard Error	6.510	6.769	6.653	9.195	9.908	10.427	10.276	14.054
Lower 95% CI	219.292	191.028	190.556	186.657	199.959	174.361	173.709	167.326
Upper 95% CI	245.281	218.049	217.116	223.367	239.524	215.998	214.742	223.446
Homo-specific intercept	NA	189.737	188.787	191.987	NA	156.877	155.739	157.393
Standard Error	NA	9.010	8.846	10.556	NA	13.729	13.505	15.825
Lower 95% CI	NA	171.753	171.131	170.917	NA	129.465	128.776	125.797
Upper 95% CI	NA	207.721	206.443	213.057	NA	184.289	182.702	188.989

Tips, data derived from species at tips of branches (conventional analysis). PICs, data derived from phylogenetically independent contrasts. Real log_{10}, log_{10} of Real branch lengths, in millions of years. Constant, all branch lengths set to 1.0. Pagel, all internode segments are set equal to one but tips are constrained to be contemporaneous. NA, not applicable.
[1]CBA4 cannot be measured in OH5.

ca. 0.75), with most animals having much more flexed basicrania than predicted by the equation (Fig. 5A). At intermediate values of IRE5, predicted (θ) and observed cranial base angles converge, except for several taxa lying below the main cluster. Ross and Henneberg (1995) suggested constraints on the upper degree of basicranial flexion. If these constraints are applied and θ is constrained to lie between 180 and 90 degrees, the distribution in Fig. 5B is obtained. The standard error of this model (18.585) is higher, but not significantly, than the standard error of the LSR (14.446).

Phylogenetic effects on basicranial flexion

Table 3 gives the LSR equations calculated from the tip data for all nonhuman euarchontans and using PICs, along with their 95% confidence limits. Equations calculated under three different branch length assumptions are presented as are *Generic* and *Homo-specific* intercept values. Results under Grafen branch lengths are omitted because they are very similar to the results using Pagel branch lengths. The LSRs are all plotted in Fig. 6. None of the LSR equations calculated using PICs differ significantly from each other in slope or intercept, so only one line is illustrated in Fig. 6. All but one (CBA4 against IRE5 under Pagel Branch lengths) of the PIC equations differed significantly from the equation using tip data. The PIC equations for CBA4 are more similar to the "tip" equations than is the CBA1 equation (Fig. 6).

Table 4 presents the *K* values for CBA1, CBA4 and IRE5 under the four different branch length assumptions. *K* values for CBA1 and IRE5 are larger than 1.0 and larger than those for CBA4, whereas *K* values for CBA4 are always smaller than 1.0. These results indicate that, relative to a Brownian motion model, closely related primates tend to resemble one another in CBA1 and IRE5 but not in CBA4.

To test whether *Homo sapiens* deviates from the allometric patterns for CBA and IRE5 across nonhuman euarchontans, PDTREE was used to calculate the prediction intervals for both measures of CBA, and for IRE5 for a new species attached to the root of the euarchontan tree (*Generic prediction intervals*) and for a new species attached to the branch leading to Sts 5 (*Homo-specific prediction intervals*). *Generic 95% prediction*

(A)

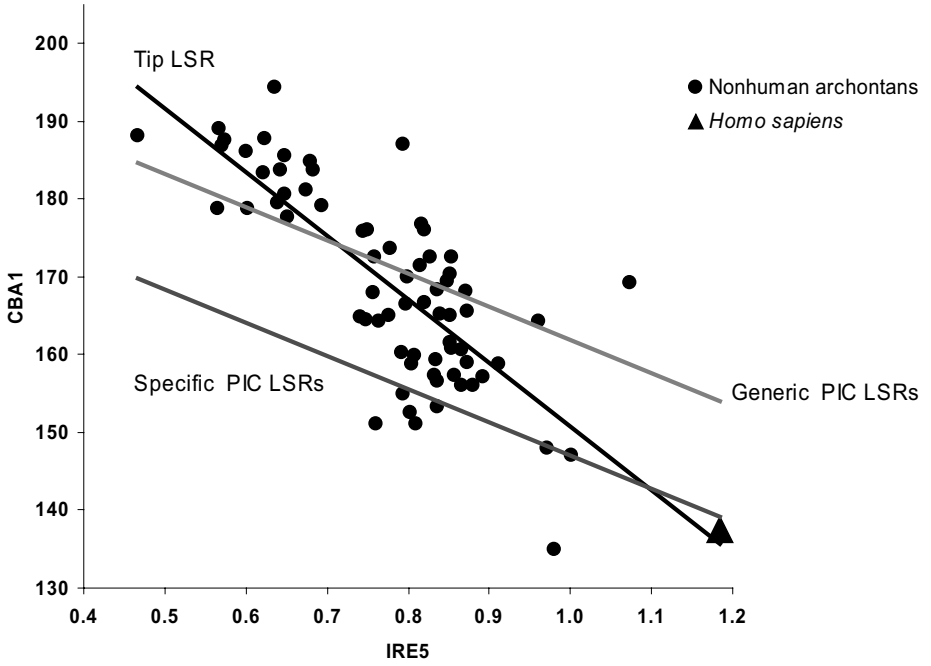
CBA1 vs IRE5
Least Squares Regressions
Tip LSR
Nonhuman archontans
Homo sapiens
Specific PIC LSRs
Generic PIC LSRs
CBA1
IRE5
200
190
180
170
160
150
140
130
0.4
0.5
0.6
0.7
0.8
0.9
1.0
1.1
1.2

(B)

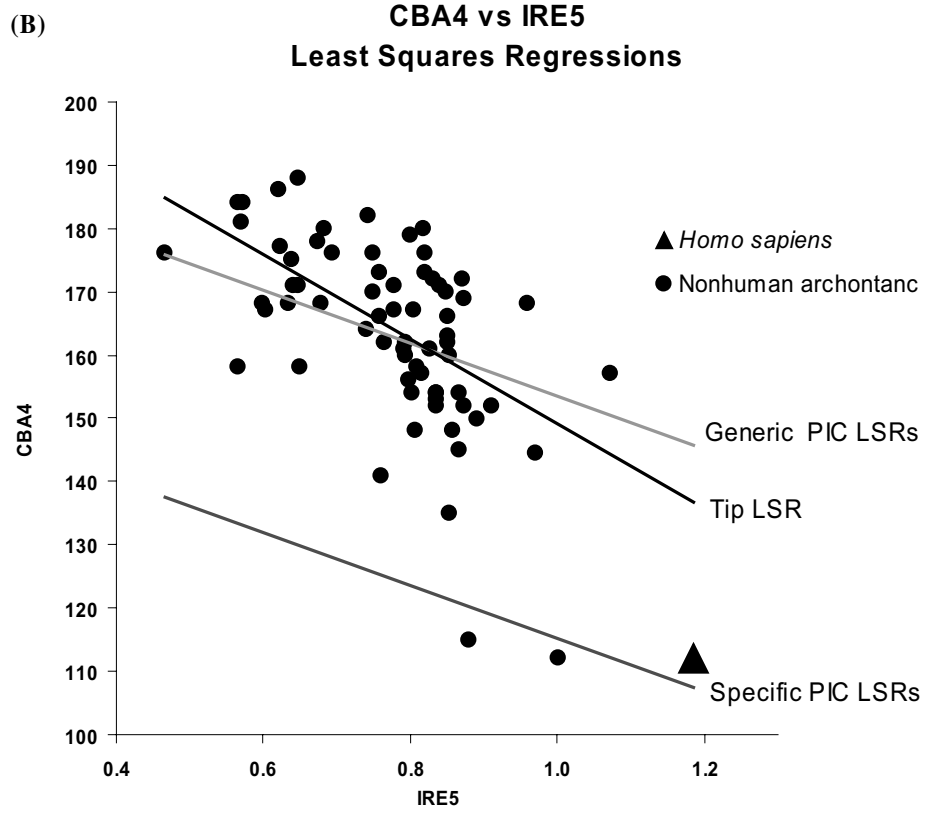
CBA4 vs IRE5
Least Squares Regressions
Homo sapiens
Nonhuman archontanc
Generic PIC LSRs
Tip LSR
Specific PIC LSRs
CBA4
IRE5
200
190
180
170
160
150
140
130
120
110
100
0.4
0.6
0.8
1.0
1.2

Table 4
Observed MSE_0/MSE, expected MSE_0/MSE and K statistic (Blomberg et al., 2003). Values calculated using all euarchontans, including *Homo sapiens*

	Real (log_{10})	Constant	Pagel	Grafen
CBA1				
K	1.500	1.486	1.237	0.280
Observed MSE_0/MSE	4.459	4.426	3.354	2.792
Expected MSE_0/MSE	2.973	2.978	2.711	9.957
CBA4				
K	0.904	0.888	0.950	0.229
Observed MSE_0/MSE	2.670	2.626	2.548	2.250
Expected MSE_0/MSE	2.949	2.957	2.682	9.814
IRE5				
K	1.555	1.487	1.050	0.262
Observed MSE_0/MSE	4.623	4.428	2.846	2.610
Expected MSE_0/MSE	2.973	2.978	2.711	9.958

intervals for IRE5 are very broad and always include the value measured for *Homo sapiens* (Table 5). The 90% PIs are narrower and only include the measured value of 1.184 under assumptions of Grafen branch lengths. The Generic 95% PIs for CBA1 and CBA4 only include the *Homo sapiens* values under assumptions of Grafen branch lengths. The Generic 90% PIs do not include the observed values.

Homo-specific prediction intervals were calculated for a species attached to the branch leading to Sts 5 (*A. africanus*) (Table 6). Once again, the 95% PIs for IRE5 are very large and always include the observed value. The 90% PIs are narrower and only include the observed values of IRE5 under assumptions of Pagel and Grafen branch lengths. The observed value for CBA1 (137.5) lay within the 95% PIs in the case of Pagel and Grafen branch lengths and within none of the 90% PIs. The observed value for CBA4 (112 degrees) lay within the 95% prediction intervals for all branch length combinations, but within none of the 90% PIs.

PDTREE was also used to determine whether the degree of flexion observed in *Homo sapiens* agrees with that predicted for a euarchontan with its relative brain size (IRE5=1.184). Once again, both *Generic* and *Homo-specific prediction intervals* were calculated, assuming a basal placement of the *Homo* branch and a placement on the branch leading to Sts 5. Table 7 lists the *Generic Prediction Intervals* for CBA1 and CBA4 for a euarchontan with an IRE5 of 1.184. The observed value of CBA1 lies within the Generic 95% PIs and CIs under Pagel and Grafen branch length assumptions only, and the observed value of CBA4 lies within the 95% CIs and PIs under Grafen branch length assumptions, and in the 95% PI under Pagel assumptions. Table 8 lists the *Homo-specific prediction intervals* for CBA1 and CBA4 for a species with an IRE5 of 1.184 attached to the branch leading to Sts 5. In all cases the observed value for CBA1 and CBA4 lie within the *Homo-specific* 95% *prediction* and *confidence intervals*.

Is basicranial flexion constrained?

To test the hypothesis that CBA4 varies as a function of IRE5, but with the degree of flexion constrained to lie between 180 and 90 degrees, various sigmoidal, polynomial, exponential, power law and quadratic functions were fit to the data for CBA4 and IRE5 gathered for this study. Equations for the best fit curves, along with the standard error of the estimate, are given in Table 9. The data are plotted in Fig. 7 along with the LSR line, the two sigmoidal curves, as well as the quadratic and Hoerl curves also found by CurveExpert. The standard error of the estimate of

Fig. 6. Bivariate plots of CBA1 and CBA4 on IRE5 and LSR lines calculated using "tips" (Tip LSR) and PICs. Generic PIC LSRs=line generated using Generic prediction method with real branch lengths (log_{10}). Specific PIC LSRs=line generated using *Homo-specific* prediction method with real branch lengths (log_{10}). Grafen, Pagel and Constant branch length lines are very similar (Table 3) and were omitted for clarity.

Table 5
Generic prediction intervals for CBA1, CBA4 and IRE5 for a new species added to the root of the euarchontan tree

Branch length assumptions	Observed	Real ($\log_{10}$)	Constant	Pagel	Grafen
Lower 95% PI for IRE5	1.184	−12.573	−11.957	−27.726	−62.046
Upper 95% PI for IRE5		13.837	13.223	29.177	63.473
Lower 90% PI for IRE5	1.184	0.476	0.481	0.432	0.083
Upper 90% PI for IRE5		0.788	0.786	1.019	1.344
Lower 95% PI for CBA1	137.5	166.509	166.889	148.502	120.299
Upper 95% PI for CBA1		188.579	187.931	196.054	225.192
Lower 90% PI for CBA1	137.5	177.413	177.283	172.033	172.219
Upper 90% PI for CBA1		177.675	177.538	172.523	173.272
Lower 95% PI for CBA4	112.0	153.185	153.587	130.777	84.764
Upper 95% PI for CBA4		184.425	183.444	198.635	245.784
Lower 90% PI for CBA4	112.0	168.674	168.387	164.459	164.779
Upper 90% PI for CBA4		168.936	168.643	164.954	165.769

Table 6
Homo-specific prediction intervals for CBA1, CBA4 and IRE5 for a new species added to the branch leading to Sts 5

Branch length assumptions	Observed	Real ($\log_{10}$)	Constant	Pagel	Grafen
Lower 95% PI for IRE5	1.184	−9.587	−9.786	−29.733	−60.901
Upper 95% PI for IRE5		11.543	11.742	31.677	62.851
Lower 90% PI for IRE5	1.184	0.853	0.848	0.655	0.354
Upper 90% PI for IRE5		1.103	1.108	1.288	1.597
Lower 95% PI for CBA1	137.5	139.136	138.963	122.467	95.901
Upper 95% PI for CBA1		156.794	156.953	173.787	199.318
Lower 90% PI for CBA1	137.5	147.861	147.849	147.863	147.090
Upper 90% PI for CBA1		148.070	148.067	148.391	148.129
Lower 95% PI for CBA4	112.0	104.081	103.780	79.607	44.202
Upper 95% PI for CBA4		128.962	129.169	153.116	185.671
Lower 90% PI for CBA4	112.0	116.417	116.366	116.094	114.413
Upper 90% PI for CBA4		116.626	116.584	116.630	115.460

the spheroid model (Equation (2)), but with $180>\theta>90$, is also given. CurveExpert found thirteen functions with lower standard errors than the LSR. Eleven of these resembled the quadratic and Hoerl curves illustrated here in being upwardly convex but without any asymptotes at low (*Homo sapiens*-like) values of CBA4. Two of the thirteen were sigmoidal with a lower asymptote lying above the value for *Homo sapiens*. None of these models has a significantly lower standard error than the LSR line as measured by an F-test. The geometric model (i.e., θ calculated from Equation (2)) performed worse than all the other models, but not significantly worse.

Discussion

The basicranial flexion data set presented here constitutes the largest yet gathered and, as such,

Table 7
Generic prediction intervals for basicranial flexion in a species with an IRE5 of 1.184

Branch lengths	Real (log_{10})	Constant	Pagel	Grafen
CBA1				
Observed CBA1	137.5	137.5	137.5	137.5
Predicted CBA1	153.958	154.410	151.580	152.207
Lower 95% CI	141.600	142.284	137.498	125.125
Upper 95% CI	166.316	166.537	165.662	179.290
Lower 95% PI	138.859	139.873	124.440	94.448
Upper 95% PI	169.058	168.947	178.719	209.966
CBA4				
Observed CBA4	112	112	112	112
Predicted CBA4	145.759	146.137	145.179	136.876
Lower 95% CI	126.720	127.405	123.554	93.531
Upper 95% CI	164.798	164.869	166.803	180.221
Lower 95% PI	122.514	123.693	103.560	45.004
Upper 95% PI	169.003	168.581	186.798	228.748

Table 8
Homo-specific prediction intervals for basicranial flexion in a species with an IRE5 of 1.184

Branch lengths	Real (log_{10})	Constant	Pagel	Grafen
CBA1				
Observed CBA1	137.5	137.5	137.5	137.5
Predicted CBA1	139.157	139.361	138.554	138.494
Lower 95% CI	133.239	133.355	131.543	131.670
Upper 95% CI	145.074	145.367	145.566	145.318
Lower 95% PI	129.268	129.343	110.804	82.270
Upper 95% PI	149.045	149.378	166.305	194.718
CBA4				
Observed CBA4	112	112	112	112
Predicted CBA4	107.456	107.650	107.185	106.650
Lower 95% CI	98.256	98.314	97.972	97.912
Upper 95% CI	116.656	116.986	116.399	115.388
Lower 95% PI	92.195	92.158	64.463	24.594
Upper 95% PI	122.717	123.142	149.908	188.706

provides an opportunity for evaluating hypotheses previously advanced in the literature. The nature of these hypotheses also provides an opportunity to evaluate the significance of some techniques for testing hypotheses in a phylogenetic context.

Is basicranial flexion adaptive or a mechanical consequence of brain enlargement?

It has been suggested that basicranial flexion might serve to accommodate increasing brain size relative to basicranial length in order to keep the shape of the brain and braincase spheroid. Both of the geometric models presented here are poor predictors of basicranial flexion and do not provide support for this hypothesis. One possibility is that primates are expanding their brains and keeping them spheroid not only by flexing the cranial base, but also by shifting the cranial base away from the centroid of the neurocranial "sphere". We evaluated this possibility by estimating the volume of brain accommodated by this displacement in the following way. For each taxon two sphere volumes were calculated, one using radius=BL2/2, and the other using radius=AP/2. The volumes of the wedges included by the degree of flexion of these taxa were calculated and the difference between the volumes of these wedges was taken to be an estimate of the increase in neurocranial volume provided by displacement of the vertex of the CBA away from the centroid of the skull. The results were even less successful than the original geometric model, suggesting that displacement does not explain the departure of the observed data from the geometrical model.

The geometrical model is probably a poor predictor of flexion because neurocranial volume is too gross a measure of brain shape. It has been demonstrated elsewhere (Ross and Ravosa, 1993; Strait, 1999; Lieberman et al., 2000) that the relative sizes of different brain parts, and of the basicranium, change interspecifically (Strait, 1999). More success is likely to be found in relating more specific aspects of brain shape to features of cranial base shape (Jeffery, 2002b). In addition, the measures used here only quantify aspects of cranial shape in the midline. Clearly brain volume and shape have effects on the size and shape of basicranial structures off the midline and future modeling should take this into account.

The sphericity explanation for basicranial flexion joins other falsified adaptive explanations for flexion (Ross and Ravosa, 1993; Strait and Ross, 1999; Lieberman et al., 2000). We therefore

Table 9
Best fit models for CBA4 vs IRE5 across all mammals studied, including *Homo sapiens*

Model name	Model structure	Coefficients	Standard error of estimate	r
Reciprocal quadratic	$y=1/(a+bx+cx^2)$	$a=0.00899118$ $b=-0.010513987$ $c=0.0086400165$	13.261	0.558
Hoerl	$y=a*(b^x)*(x^c)$	$a=945.82188$ $b=0.14927051$ $c=1.0600076$	13.346	0.550
Quadratic fit	$y=a+bx+cx^2$	$a=110.40289$ $b=206.24765$ $c=-174.47529$	13.350	0.550
Weibull	$y=a-b*\exp(-c*x^d)$	$a=170.77789$ $b=64.538633$ $c=0.71028155$ $d=-5.0852365$	13.306	0.551
MMF	$y=(a*b+c*x^d)/(b+x^d)$	$a=125.40573$ $b=2.8048554$ $c=170.893$ $d=-12.284483$	13.418	0.544
Linear fit	$y=a+bx$	$a=193.9582$ $b=-41.921816$	14.446	0.426
Spheroid model (Equation (2))	$\theta=\left\{2\pi-\frac{3}{2r^3}V\right\}$ where $(180>y>90)$		18.585	

conclude that basicranial flexion is not adaptive, but is a mechanical "spatial packing" effect of enlargement of the brain relative to basicranial length, and/or enlargement of the cerebrum relative to the brainstem (Ross and Ravosa, 1993; Strait, 1999). Jeffery (1999) and Jeffery and Spoor (2002) argued against this hypothesis because they found that increases in relative brain size during prenatal ontogeny in humans were actually accompanied by decreases rather than increases in flexion. However, consideration of the range of ontogenetic changes in flexion and relative brain size in the context of the interspecific data suggests that the spatial packing hypothesis still explains much of the variance in basicranial flexion. Fig. 8 plots all of the available ontogenetic and interspecific data on CBA1 and IRE5. Species means for the adult primates and nonprimate mammals are given in Table 2; data on fetal *Homo* come from Jeffery (1999), and data from fetal *Macaca nemestrina* and *Alouatta caraya* are from Jeffery (2003), courtesy of the author. It is apparent that at any relative brain size there is a wide range of variability in the degree of basicranial flexion, some of which is evident during ontogeny and some of which is apparent in interspecific comparisons of adults. Given this variability, it is not surprising that humans cannot be definitively shown to deviate from the relationship seen in other taxa (Fig. 8). However, even when this variability is taken into account, there is still a significant relationship between relative brain size and basicranial flexion in interspecific comparisons. Clearly prenatal ontogenetic trajectories in basicranial flexion and relative brain size can run counter to the spatial packing model, but only within the limits of the general trend. Consequently, we believe that it is still reasonable to suggest that much of the variance in basicranial flexion is a mechanical consequence of increasing relative brain size, even in the context of the accumulating ontogenetic data.

It is interesting that, although cranial bases retroflex with increasing relative brain size within

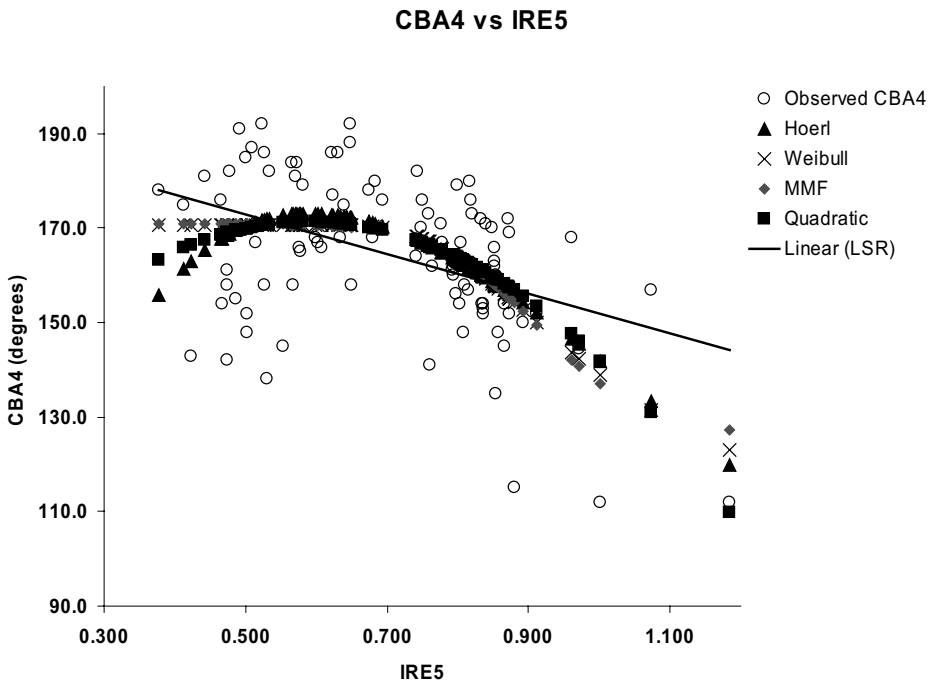

Fig. 7. Bivariate plot of CBA4 against IRE5 across all taxa sampled in this study. LSR line also illustrated, along with values for CBA4 predicted by selected equations from Table 9. The values predicted by two sigmoidal functions, MMF and Weibull, are illustrated, along with a power law function (Hoerl) and the quadratic equation.

fetal samples of *Homo sapiens*, *Macaca nemestrina* and *Alouatta caraya* (Jeffery, 1999; Jeffery and Spoor, 2002; Jeffery, 2003) (Fig. 8), the postnatal ontogeny of *Homo sapiens* differs from that of the other taxa (Sirianni and Swindler, 1979). If the adult congenerics of *Alouatta* (*palliata* and *belzebul*) and *Macaca* (*fascicularis*, *nigra*, *sylvana*) are any indication, their postnatal ontogeny witnesses decreases in relative brain size presumably as cranial base growth outpaces that of the brain. In contrast, in *Homo sapiens* brain growth continues to outpace basicranial growth postnatally. It remains to be determined what factors other than relative brain size cause the cranial base to retroflex in the prenatal period, and why humans do not follow the general primate postnatal ontogenetic pattern.

Several nonprimate mammals exhibit basicrania that are highly flexed for their relative brain size, regardless of the regression equation used (Fig. 5b, Fig. 7). These include lagomorphs, most bovids, and one bat, *Pteropus hypomelanus*. The most highly flexed basicrania among nonprimate mammals are found among lagomorphs. DuBrul suggested that orthograde lagomorphs, such as *Lepus*, possess a suite of features—including a more highly flexed basicranium—not seen in more pronograde lagomorphs, such as *Ochotona* (DuBrul, 1950). This study does not support DuBrul's suggestion: *Lepus* has a mean CBA4 of 148 degrees and mean CBA1 of 186 degrees, while those of *Ochotona* are 143 and 172 respectively. DuBrul assumed that orthograde mammals have more flexed basicrania because they have more vertically aligned cervical vertebral columns, but this assumption is incorrect. Radiographic studies reveal that rats, cats, rabbits, guinea pigs, monkeys and humans all have vertically oriented cervical vertebral columns when at rest, despite a wide range of postures and basicranial flexion (Vidal et al., 1986). Thus, the flexed basicrania of lagomorphs are not related to their neck posture, a

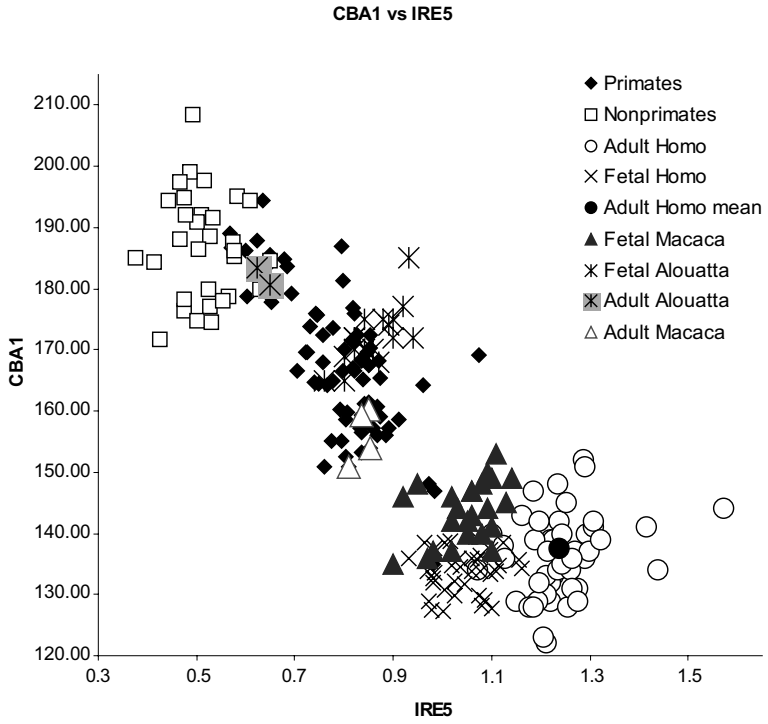

Fig. 8. Plot of primate and non-primate data on CBA1 and IRE5. Adult species means from this paper; *Homo* fetal data from Jeffery (1999); *Macaca* and *Alouatta* fetal data from Jeffery (2003).

conclusion also drawn for primates (Strait and Ross, 1999).

One possibility is that basicranial flexion in lagomorphs is associated with ventral deflection, or kyphosis, of the face. As Dabelow (1929, 1931) suggested, animals with their orbits closely approximated to the midline show a close correlation between orbit orientation and basicranial flexion because the orbits become structurally integrated with the anterior cranial base (Ross and Ravosa, 1993; Ross and Henneberg, 1995). Lagomorphs have closely approximated orbits, suggesting that basicranial flexion in these animals may be associated with their strong facial kyphosis. Facial kyphosis in turn may function to move the rostrum below the level of the horizon so that lagomorphs can scan the world anteriorly when in an "alert" posture. The validity of this hypothesis remains to be evaluated.

The four species of small bovids measured for this study also have moderately flexed basicrania. Endocranial flexion in bovids has not been studied previously, although externally measured flexion of the face on the braincase has been attributed to a need to decrease the length of the head to reduce torques due to gravity (Gentry, 1980), as a means of orienting the head properly for head-butting combat (Schaffer and Reed, 1972) and as a correlate of grass feeding, particularly in secondary grasslands (Spencer, 1995). It is not clear that the flexion of the face on the braincase referred to by these authors is linked to endocranial flexion, although the highly approximated orbits of the small bovids measured here suggests that it might be. However, the "head-butting" hypothesis is unlikely to be correct in these small bovids, all of which have small heads and none of which are reported to engage in head-butting combat. Whether the relationships observed by Spencer also hold when endocranial basicranial flexion is measured remains to be shown, however, the small bovids measured for this study all feed to some degree on grasses.

Phylogenetic effects on basicranial flexion

The recent development of methods for taking phylogenetic relatedness into account when analyzing comparative data makes it possible to evaluate the influence of phylogeny on patterns of relationship between measures of relative brain size and basicranial flexion. Comparison of LSR equations calculated using tip data with those calculated using PICs reveals significant phylogenetic effects on the relationship between both measures of flexion and measures of relative brain size (Table 3, Fig. 6). Thus, phylogeny needs to be taken into account in evaluating hypotheses regarding flexion.

The effect of the four different branch length sets on the slopes and intercepts of the PIC equations are minimal. However, there were some differences in the prediction and confidence intervals calculated under the four branch length assumption sets. The prediction and confidence intervals generated by the Pagel and Grafen branch lengths are much wider than those under constant or real ($\log_{10}$) branch lengths, accounting for some differences in results between branch length sets. These results suggest that sensitivity analyses using different branch length sets are advisable when making predictions, but may be less important when calculating slopes and intercepts within Primates.

Notably the LSR slopes calculated using the tip data for CBA4 are close to the 95% CIs for the LSR slopes calculated using PICs under real ($\log_{10}$) and constant branch lengths, and are included in the 95% CIs under Grafen branch lengths. CBA4 is apparently less influenced by phylogeny than CBA1. This conclusion is supported by the *K* statistics reported in Table 4. The fact that *K* values for CBA1 are always larger than 1.0, and those for CBA4 are always smaller than 1.0 suggests that closely related primates tend to resemble one another in CBA1 more closely than if they were placed on the tips of the tree at random. In contrast, closely related primates do not tend to resemble one another in CBA4 more than would be predicted at random. The most salient difference between these measures is the anterior point on the anterior cranial base—foramen caecum in CBA1 and anterior edge of planum sphenoideum (PS) in CBA4. It may be that the position of foramen caecum is more strongly influenced by the morphology of the face than is the position of PS, and that facial morphology is more strongly associated with phylogeny. Further research into phylogenetic effects on the angles of orbit and palate orientation would evaluate this hypothesis.

Garland and Ives (2000) present two distinctly different kinds of prediction intervals that can be calculated using their software, PDTREE. In both cases PICs are used to calculate the slope and intercept of the LSR line. *Generic prediction intervals* are so-called because they do not specify the position of the hypothetical species for which values are to be predicted very precisely. Consequently, the LSR line is calculated as running through the estimated root node values for the tree. Obviously the position of the hypothetical taxon attaching to the root node is as specific as any other position in the tree, so "generic" is something of a misnomer. However, the predictions are generic in the sense of applying to all the descendents of the root node. *Homo-specific prediction intervals* were also calculated in this study, with *Homo sapiens* attaching to the branch leading to Sts 5, *Australopithecus africanus*. In these cases the slope of the LSR line is identical to the line used for *Generic predictions*, but the intercept is very different (Table 3, Fig. 6), more closely approximating the value for Sts 5. A helpful way of thinking about these two approaches to prediction is to imagine oneself armed with knowledge of the slope of the relationship between basicranial flexion and relative brain size, standing at the root node of the euarchontan tree in the *Generic* case, and at the *Homo sapiens–Australopithecus africanus* node in the *Homo-specific* case. Knowing the values for IRE5 and basicranial flexion at those nodes and the slope of the relationship between them enables one to predict their respective values 83 Myr from that node in the *Generic* case (Fig. 6, "*Generic* LSRs"), and 4 Myr from that node in the *Homo-specific* case (Fig. 6 "*Homo-specific* LSRs"). The predicted values are given in Tables 5 and 6. If one were also armed with prior knowledge of the IRE5 value at the ends of those two branches, one could also predict the CBA

values there. These predicted values are given in Tables 7 and 8.

In this study, predictions were made under four different branch length assumptions in order to document the sensitivity of the results to these assumptions. Using the *Generic prediction intervals* (Table 5), the human IRE5 is included in all the 95% prediction intervals (which are very broad) but is only included in the 90% prediction intervals under Grafen branch lengths. This suggests that the relatively large brains of humans are unusual in the context of euarchontans in general (see also Fig. 6). In the *Homo-specific* case, the IRE5 of *Homo sapiens* fell within the 90% prediction intervals using Pagel and Grafen branch lengths and very close to the upper limit of the 90% prediction interval for real (log) and constant branch lengths. This suggests that the relative brain size of modern humans is less unusual in a taxon attached to the branch leading to *A. africanus*.

When cranial base flexion measures are considered, under the *Generic prediction intervals* the degree of flexion seen in the human cranial base cannot be predicted simply from knowledge of the distribution of flexion amongst euarchontans (Table 5). One needs more specific knowledge regarding the placement of humans within Euarchonta. When this is provided, the CBA4 value for *Homo sapiens* falls within the 95% prediction intervals under most branch length assumption sets (Table 6), whereas the CBA1 value is only predicted under Pagel and Grafen assumption sets. It would seem that the CBA1 of anatomically modern humans is unusual, even in the context of closely related hominins. Specifying the relative brain size (IRE5) of the species for which flexion is to be predicted produces slightly better results, particularly for estimates of CBA1 (Table 7). However, it is not until both IRE5 and the phylogenetic position of *Homo sapiens* are specified that the degree of flexion observed for *Homo sapiens* is consistently included within 95% prediction and confidence intervals for all branch length sets (Table 8).

In order to more precisely identify the point on the phylogenetic tree when the degree of flexion and relative brain size in *Homo* become predictable, some additional analyses were run. Using PDTREE, the phylogenetic tree was successively rerooted at the ancestral nodes for Hominoidea, the last common ancestor of the *Pan–Homo* clade, and the last common ancestor of the *Homo–Paranthropus* clade and the 95% prediction and confidence intervals for IRE5, CBA1, and CBA4 were calculated for a species attached to these nodes by branch lengths equal to the age of the nodes ($\log_{10}$). Results reveal that at the hominoid node the CBA1 and CBA4 of *Homo sapiens* are not predictable, even if the IRE5 of 1.184 is specified. At the node representing the last common ancestor of *Homo* and *Pan*, the CBA1 and CBA4 of *Homo sapiens* are not predictable without specifying the IRE5 of *Homo sapiens*. When this is specified the CBA1 of *Homo sapiens* is predictable, falling within the 90% confidence limits, but the CBA4 is only barely predictable, falling within the 90% prediction intervals but outside the 90 and 95% confidence intervals. In light of the unusually rapid increase in both relative brain size and basicranial flexion, it seems reasonable that the degree of flexion in *Homo sapiens* is only predictable at the *Pan–Homo* node when information on IRE5 is available.

At the node representing the last common ancestor of *Paranthropus* (OH5+KNM WT 17000) and *Homo sapiens*, CBA1 is not predictable unless the IRE5 of *Homo sapiens* is specified, but CBA4 is predicted even without this information. This difference reflects the fact that the CBA4s of *Homo sapiens*, OH5, KNM WT 17000 and Sts 5 are all very similar (and lower than those of the extant apes), whereas the CBA1s of OH5 5 and *Homo sapiens* are lower than those of great apes, KNM WT 17000 and Sts 5. As noted above, the difference between CBA1 and CBA4 inheres principally in the position of foramen cecum relative to the planum sphenoideum. The low CBA1s of KNM WT 17000 and great apes relative to their CBA4s might reflect the fact that their faces are hafted high on the neurocranium, implying that foramen cecum is part of a facial "module", rather than a more posteriorly located "basicranial module" which includes planum sphenoideum (*sensu* McCollum, 1999). In this light it is worth noting that the extant hominoids have been shown to have airorhynch orbits and palates (Ross and Henneberg, 1995), which might be associated with

dorsal deflection of the foramen cecum relative to the rest of the cranial base.

Is basicranial flexion constrained?

Constraint on the degree of basicranial flexion (CBA4) in *Homo sapiens* was originally suggested because humans fall outside the 95% confidence limits of the RMA line calculated for other primates (Ross and Henneberg, 1995). Does *Homo sapiens* really have a less flexed basicranium than expected for their relative brain size? It depends on your vantage point. The degree of flexion in *Homo sapiens* is not predictable for a taxon attached to the ancestral hominoid node by a branch 16 Myr long, but it is predictable for a euarchontan of its relative brain size attached to the branch leading to Sts 5 by a branch 4 Myr long. This suggests that the closer one gets to the corner of morphospace in which humans are found, the more reasonable their basicranial anatomy becomes. Moreover, the fact that the degree of flexion in humans is only predictable from the vantage of the last common ancestor of *Homo sapiens* and *Paranthropus* seems to suggest that *Homo* occupies an unusual corner of morphospace not directly accessible from all parts of the primate tree. But it does not speak directly to the issue of whether the degree of flexion in *Homo sapiens* is constrained or not. Because the application of PICs to curvilinear regression in the original data space is not yet possible, this question can only be addressed using tip data.

Although none of the curvilinear models produced a significantly better fit than the simple linear LSR, many of them did have lower standard errors, including two sigmoidal curves (MMF and Weibull) with asymptotes at higher levels of IRE5. Thus, these results leave open the possibility that one of the nonlinear equations will ultimately best describe the relationship between relative brain size and flexion. Indeed, although the differences between these models are not significant, the curvilinear models perform better than the simple LSR. No theoretical reasons have yet been advanced for preferring rectilinear over curvilinear models of the relationship between flexion and relative brain size, and the hypothesis of constraint is at least as powerful as an ordinary rectilinear model in modeling the relationship between flexion and relative brain size.

One possible reason for the lack of resolution of this issue is the lack of data on basicranial flexion and relative brain size for hominids more closely related to *Homo sapiens* than *Australopithecus africanus*. If these taxa are found to have values of CBA4 similar to *Homo sapiens*, OH5, KNM WT 17000 and Sts 5, this will provide further support for the curvilinear models. If, however, they have great ape-like values of CBA4, the rectilinear models will gain support.

Evolution of basicranial flexion and relative brain size in primates

Using PDTREE it is possible to estimate the values for IRE5, CBA1 and CBA4 at the internal nodes in the phylogeny in Fig. 3. The estimated values, ± 1 standard error, for the Euarchonta, Primates, Haplorhini, Anthropoidea, Catarrhini, Hominoidea and Homininae nodes are plotted in Fig. 9 against the age of the node in Myr. The values, plus the 95% confidence intervals, are given in Table 10. Brain size increases are evident between the euarchontan and primate nodes, with the primate IRE5 values lying more than one standard error above the euarchontan value. Further increases in IRE5 occur at all subsequent nodes, but in all but one case the value for each node lies within one standard error of the preceding node. The only exception is that of the *Homo sapiens–Australopithecus africanus* clade, which evinces a massive increase in IRE5 in a relatively short period of time (16–6 Myr).

The two basicranial flexion measures display similar, but not identical patterns of change in primate phylogeny. Basicranial flexion increases notably (i.e., CBA values decrease) along the primate stem concurrent with the rapid increases in IRE5. However, whereas IRE5 only shows minor increases along the lineage leading to haplorhines, basicranial flexion measures show marked changes. Both CBA1 and CBA4 increase slightly at the Anthropoidea node before decreasing in the ancestral Catarrhini node. In the lineage leading to the ancestral Hominoidea node CBA4 decreases whereas CBA1 does not; both measures show

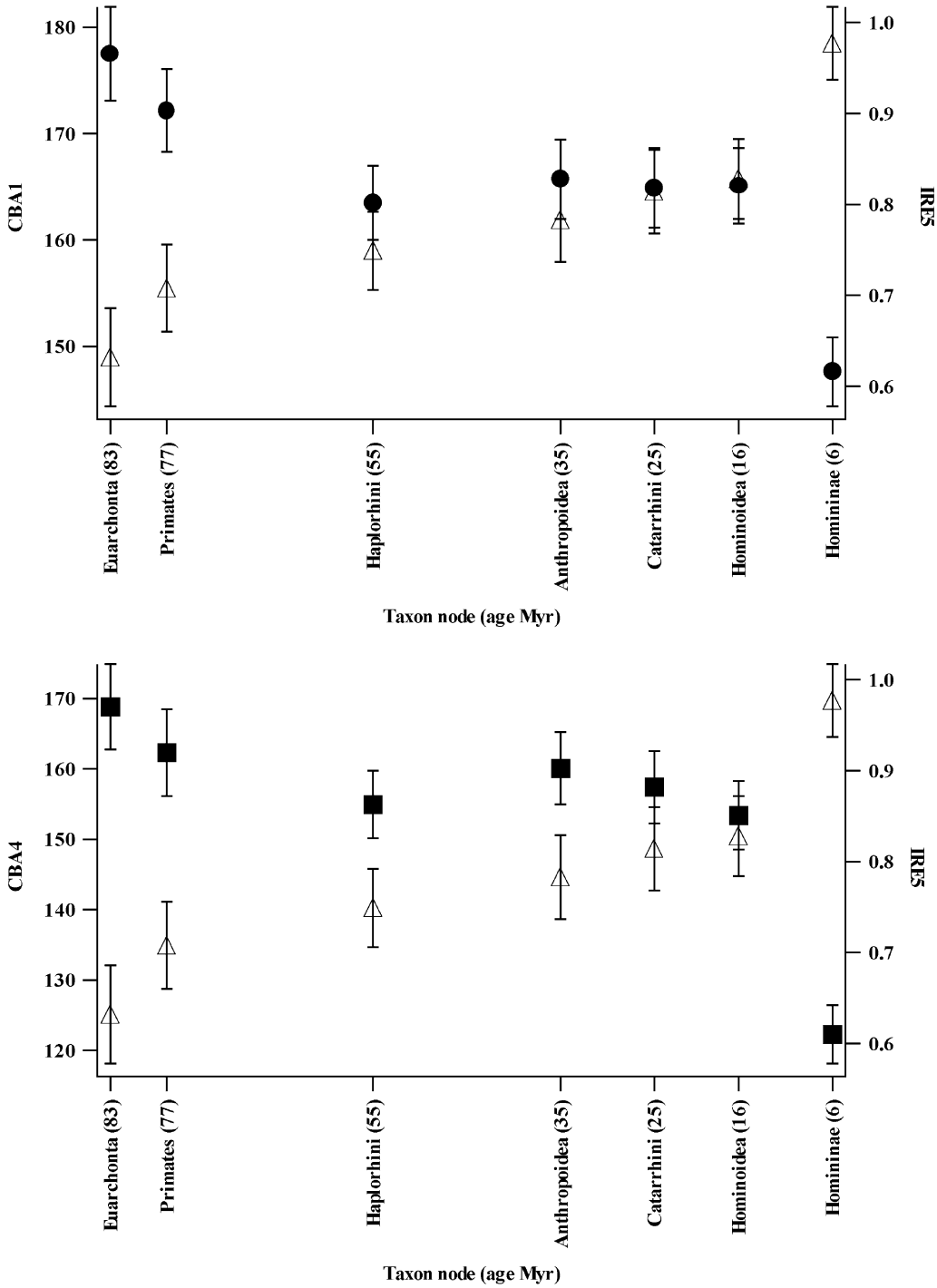

Fig. 9. Bivariate plot of estimated values of CBA1 and IRE5 (top) and CBA4 and IRE5 (bottom) at selected nodes from the phylogenetic tree in Fig. 3. Error bars are ±standard error. 95%CI are very wide and are given in Table 10.

Table 10
Estimates of CBA1, CBA4 and IRE5 at selected internal nodes in the tree from Figure 3

Node	Age (Myr)	CBA1				CBA4				IRE5			
		Value	Std error	Upper 95%	Lower 95%	Value	Std error	Upper 95%	Lower 95%	Value	Std error	Upper 95%	Lower 95%
Euarchonta	83	177.5	4.41	186.3	168.8	168.807	6.054	180.886	156.727	0.632	0.054	0.740	0.524
Primates	77	172.2	3.88	180.0	164.5	162.309	6.166	172.944	151.675	0.708	0.048	0.804	0.613
Haplorhini	55	163.5	3.49	170.5	156.6	154.951	4.794	164.518	145.385	0.749	0.043	0.834	0.663
Anthropoidea	35	165.7	3.75	173.2	158.2	160.077	5.149	170.351	149.802	0.783	0.046	0.875	0.691
Catarrhini	25	164.9	3.74	172.4	157.4	157.422	5.139	167.676	147.168	0.814	0.046	0.906	0.722
Hominoidea	16	165.1	3.56	172.2	158.0	153.391	4.894	163.157	143.625	0.828	0.044	0.915	0.740
Pan–Homo	6	147.6	3.25	154.1	141.2	122.294	4.158	130.591	113.996	0.977	0.040	1.056	0.897

rapid decreases in the lineage leading to the last common ancestor of *Homo sapiens* and *Australopithecus africanus*.

Many of these changes are probably not significant as the 95% confidence intervals at all nodes are very broad. Nevertheless, this framework of relative brain size and flexion evolution in primates is a hypothesis for future testing as data for more fossil taxa become available.

Conclusions

Previous work has indicated that the degree of basicranial flexion in primates is correlated with relative brain size, that humans might be less flexed than predicted for their relative brain size, and that this might suggest that the degree of flexion in relatively large brained species is constrained (Ross and Ravosa, 1993; Ross and Henneberg, 1995). It had also been suggested that flexion might enable the brain to maintain a spheroid shape while increasing in relative size (Lieberman et al., 2000). Evaluating these hypotheses in a phylogenetic context reveals that whether humans have a less flexed basicranium than expected for their relative brain size depends on your vantage point. They are not less flexed than expected for a descendent of the last common ancestor of the *Paranthropus–Homo* clade, but their degree of flexion cannot be predicted from the basal hominoid and higher nodes, even if their relative brain size is specified. Humans undoubtedly occupy an unusual part of morphospace in terms of basicranial flexion and relative brain size, but this does not mean that their degree of flexion is or is not constrained. Curvilinear modeling describes the relationship between flexion and relative brain size at least as well as, and sometimes better than, simple linear least squares regression, suggesting that the hypothesis of constraint cannot be falsified at present. The hypothesis that basicranial flexion is an adaptation to maintain a spheroid brain shape receives no support in this analysis. Rather, much of the variance in basicranial flexion can reasonably be hypothesized to be a mechanical consequence of increases in relative brain size, although other influences on flexion in postnatal ontogeny are suggested by the work of Jeffery and Spoor (2002).

Acknowledgements

We thank Matt Cartmill and Dan Lieberman for access to x-rays in their care and Dan Lieberman for the generous loan of an x-ray machine. Rob McCarthy and Kenneth Mowbray assisted in x-raying of specimens. The staff of the AMNH, including the late Wolfgang Fuchs, BMNH, Field Museum and British Museum (Natural History) provided access to specimens in their care. Brigitte Demes, Dan Lieberman, Fred Spoor and three anonymous reviewers provided insightful comments on the manuscript. Bill Jungers and Ted Garland tendered statistical advice. Ted Garland provided PDAP and PHYSIG.M software. Nathan Jeffery and Fred

Spoor kindly provided unpublished data that improved the manuscript. Luci Betti-Nash assisted with the illustrations.

Appendix A. Derivation of equation 1

Area of circle:

$$A=\pi r^2$$

Area of partial circle:

$$A=r^2\left\{\pi-\frac{\theta}{2}\right\}$$

Volume (V) of sphere:

$$V=\frac{4}{3}\pi r^3$$

Volume (V) of partial sphere:

$$V=\frac{2r^3}{3}\{2\pi-\theta\}$$

Rearranged yields Equation 1

$$\theta=\left\{2\pi-\frac{3}{2r^3}V\right\}$$

References

Allman, J.M., Kaas, J.H., 1974. The organization of the second visual area (V II) in the owl monkey: a second order transformation of the visual hemifield. Brain Res. 76, 247–265.

Barlow, H.B., 1986. Why have multiple cortical areas? Vision Res. 26, 81–90.

Blomberg, S.P., Garland, T.G. Jr, Ives, A.R., 2003. Testing for phylogenetic signal in comparative data: behavioral traits are more labile. Evolution 57, 717–745.

Chaves, R., Sampaio, I., Schneider, M.P., Schneider, H., Page, S.L., Goodman, M., 1999. The place of *Callimico goeldii* in the callitrichine phylogenetic tree: evidence from von Willebrand factor gene intron II sequences. Mol. Phylo-Genet. Evol. 13, 392–404.

Cherniak, C., 1995. Neural component placement. Trends Neurosci. 18, 522–527.

Dabelow, A., 1929. Über Korrelationenin der phylogenetischen Entwicklung der Schädelform. Gegenbaurs Morphol Jahrb 63, 1–49.

Dabelow, A., 1931. Über Korrelationenin der phylogenetischen Entwicklung der Schädelform. II. Die Beziehungen zwischen Gehirn und Schädelbasisform bei den Mammaliern. Gegenbaurs Morphol Jahrb 67, 84–133.

Demes, A.B., 1985, Biomechanics of the Primate Skull Base. Advances in Anatomy, Embryology and Cell Biology. 94. Springer-Verlag, Berlin.

DuBrul, E.L., 1950. Posture, locomotion and the skull in Lagomorpha. Am. J. Anat. 87, 277–313.

Eizirik, E., Murphy, W.J., Springer, M.S., O'Brien, S.J., 2003. Molecular phylogeny and dating of early primate divergences. In: Ross, C.F., Kay, R.F. (Eds.), Anthropoid Origins: New Visions. Kluwer Academic/Plenum Publishers, New York, pp. 45–64.

Felsenstein, J., 1985. Phylogenies and the comparative method. Am. Nat. 125, 1–15.

Garland, T. Jr, Harvey, P.H., Ives, A.R., 1992. Procedures for the analysis of comparative data using phylogenetically independent contrasts. Systematic Biology 41, 18–32.

Garland,T. Jr, Midford, P.E., Jones, J.A., Dickerman, A.W., Diaz-Uriarte, R., PDAP: Phenotypic Diversity Analysis Programs. Version 6.0 Copyright March 2002.

Garland, T. Jr, Midford, P.E., Ives, A.R., 1999. An introduction to phylogenetically based statistical methods, with a new method for confidence intervals on ancestral states. Am. Zool. 39, 374–388.

Garland, T. Jr, Dickerman, A.W., Janis, C.M., Jones, J.A., 1993. Phylogenetic analysis of covariance by computer simulation. Syst. Biol. 42, 265–292.

Garland, T. Jr, Ives, A.R., 2000. Using the past to predict the present: Confidence intervals for regression equations in phylogenetic comparative methods. American Naturalist 155, 346–364.

Gentry, A.W., 1980. Fossil Bovidae (Mammalia) from Langabaanweg. Annls S. Afr. Mus. 79, 213–337.

Gould, S.J., 1977. Ontogeny and Phylogeny. Belknap Press, Cambridge.

Grafen, A., 1989. The phylogenetic regression. Phil. Trans. R. Soc. Lond. B 326, 119–157.

Hartwig, W.C., 2002. The Primate Fossil Record. Cambridge University Press, Cambridge.

Jablonski, N.G., 2002. Fossil Old World monkeys: The late Neogene radiation. In: Hartwig, W.C. (Ed.), The Primate Fossil Record. Cambridge University Press, Cambridge, pp. 255–299.

Jeffery, N., 1999. Fetal Development and Evolution of the Human Cranial Base. Ph.D. Thesis, University College London.

Jeffery, N., 2002a. A high-resolution MRI study of linear growth of the human fetal skull base. Neuroradiology 44(4), 358–366.

Jeffery, N., 2002b. Differential regional brain growth and rotation of the prenatal human tentorium cerebelli. J. Anat. 200, 135–144.

Jeffery, N, 2003. Brain expansion and comparative prenatal ontogeny of the non-hominoid cranial base. J. Hum. Evol. 45, 263–284.

Jeffery, N., Spoor, F., 2002. Brain size and the human cranial base: a prenatal perspective. Am. J. Phys. Anthrop. 118(4), 324–340.

Lieberman, D.E., McCarthy, R.C., 1999. The ontogeny of cranial base angulation in humans and chimpanzees and its implications for reconstructing pharyngeal dimensions. J. Hum. Evol. 36, 487–517.

Lieberman, D.E., Ross, C.F., Ravosa, M.J., 2000. The primate cranial base: Ontogeny, function and integration. Yearb. Phys. Anthrop. 43, 117–169.

McCarthy, R., 2001. Anthropoid cranial base architecture and scaling relationships. J. Hum. Evol. 40, 41–66.

McCollum, M.A., 1999. The robust australopithecine face: A morphogenetic perspective. Science 284, 301–305.

Mitchison, G., 1991. Neuronal branching patterns and the economy of cortical wiring. Proc. R. Soc. Lond. B 245, 151–158.

Murphy, W.J., Eizirik, E., Johnson, W.E., Zhang, Y.P., Ryder, O.A., O'Brien, S.J., 2001. Molecular phylogenetics and the origins of placental mammals. Nature 409, 614–618.

Page, S.L., Chiu, C., Goodman, M., 1999. Molecular phylogeny of Old-World Monkeys (Cercopithecidae) as inferred from γ-globin DNA sequences. Mol. Phylogenet. Evol. 13, 348–359.

Pagel, M.D., 1992. A method for the analysis of comparative data. J. Theoret. Biol. 156, 431–442.

Porter, C.A., Page, S.L., Czelusniak, J., Schneider, H., Schneider, M.P.C., Sampaio, I., Goodman, M., 1997. Phylogeny and evolution of selected primates as determined by sequences of the ε-globin locus and 5′ flanking regions. Int. J. Primatol. 18, 261–295.

Rohlf, J., 2002. Comparative methods for the analysis of continuous variables: Geometric interpretations. Evolution 55, 2143–2160.

Ross, C.F., 2003. Review of "The Primate Fossil Record" Edited by Walter C. Hartwig. J. Hum. Evol. 45, 195–201.

Ross, C.F., Ravosa, M., 1993. Basicranial flexion, relative brain size and facial kyphosis in nonhuman primates. Am. J. Phys. Anthrop. 91, 305–324.

Ross, C.F., Henneberg, M., 1995. Basicranial flexion, relative brain size and facial kyphosis in *Homo sapiens* and some fossil hominids. Am. J. Phys. Anthrop. 98, 575–593.

Schaffer, W.M., Reed, C.A., 1972. The coevolution of social behavior and cranial morphology in sheep and goats (Bovidae, Caprini). Fieldiana Zoology 61, 1–88.

Seiffert, E.R., Simons, E.L., Attia, Y., 2003. Fossil evidence for ana ncient divergence of losies and galagos. Nature 422, 421–424.

Sirianni, J.E., Swindler, D.R., 1979. A review of postnatal craniofacial growth in Old World Monkeys and Apes. Yearb. phys. Anthrop 22, 80–104.

Smith, R.J., 1994. Degrees of freedom in interspecific allometry: an adjustment for the effects of phylogenetic constraint. Am. J. Phys. Anthrop. 93, 95–107.

Sokal, R.F., Rohlf, F.J., 1981Biometry, WH Fremman and Co, New York.

Spencer, L.M., 1995. Antelopes and Grasslands: Reconstructing African Hominid Environments. Ph.D. Dissertation, SUNY at Stony Brook.

Spoor, F., 1997. Basicranial architecture and relative brain size of Sts 5 (*Australopithecus africanus*) and other Plio-Pleistocene hominids. S. Afr. J. Sci. 93, 182–186.

Strait, D., 1999. The scaling of basicranial flexion and length. J. Hum. Evol. 37, 701–719.

Strait, D., Ross, C.F., 1999. Head posture, neck posture, relative brain size and the evolution of basicranial flexion. Am. J. Phys. Anthrop. 108, 205–222.

Van Essen, D.C., 1997. A tension-based theory of morphogenesis and compact wiring in the central nervous system. Nature 385, 313–318.

Vidal, P.P., Graf, W, Berthoz, A, 1986. The orientation of the cervical vertebral column in unrestrained awake animals. I. Resting position. Exp Brain Res 61, 549–559.

Yoder, A.D., Cartmill, M., Ruvolo, M., Smith, K., Vilgalys, R., 1996. Ancient origin for Malagasy primates. Proc. Natl. Acad. Sci. 93, 5122–5126.

Yoder, A.D., 1997. Back to the future: A synthesis of strepsirrhine systematics. Evol. Anthrop. 6, 11–22.

Zuckerman, S., 1955. Age changes in the basicranial axis of the human skull. Am. J. Phys. Anthrop. 13, 521–539.